

Q C D @ W O R K — LECCE, June 27th, 2022

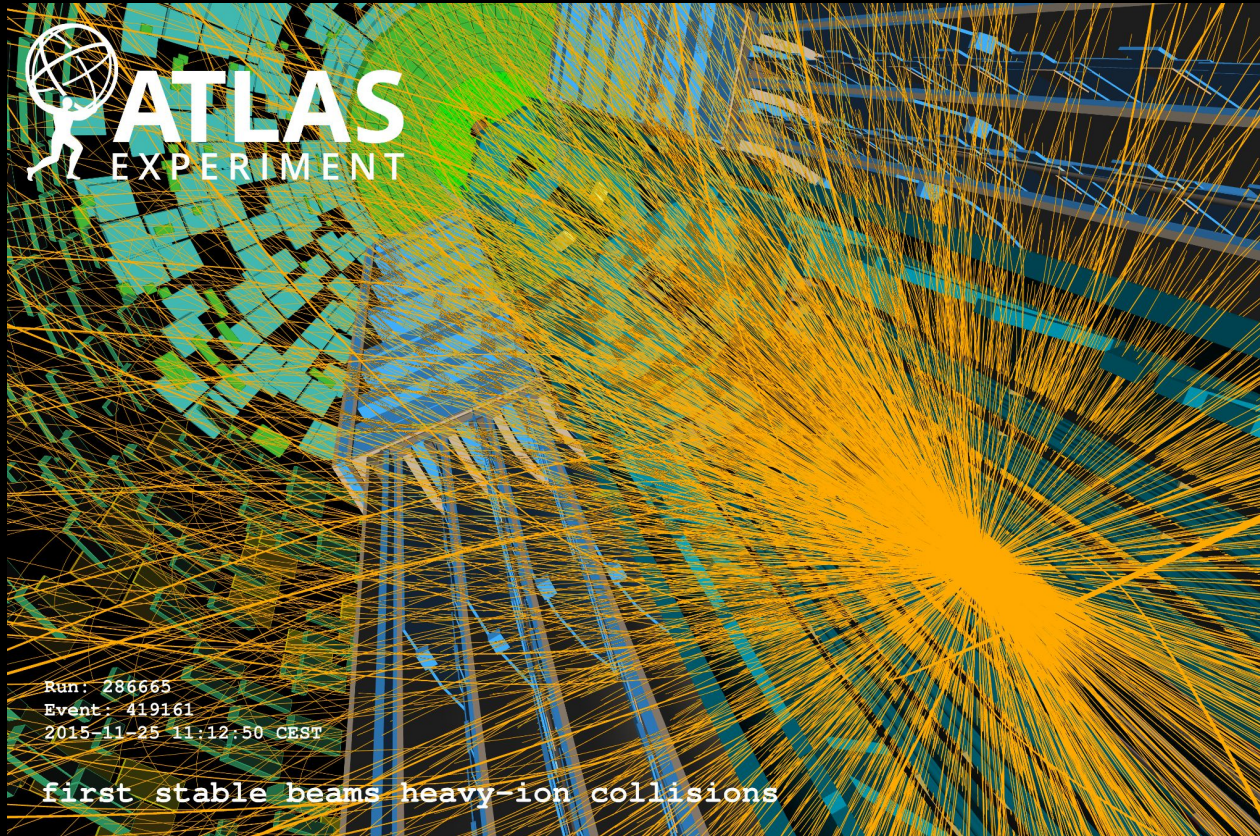
Measuring QCD in its extremes at ATLAS

Ynyr Harris (University of Oxford) on behalf of the ATLAS Collaboration



Extreme QCD happens at the LHC

In high multiplicity pp, p+Pb, and Pb+Pb collisions — little bangs producing big bang matter

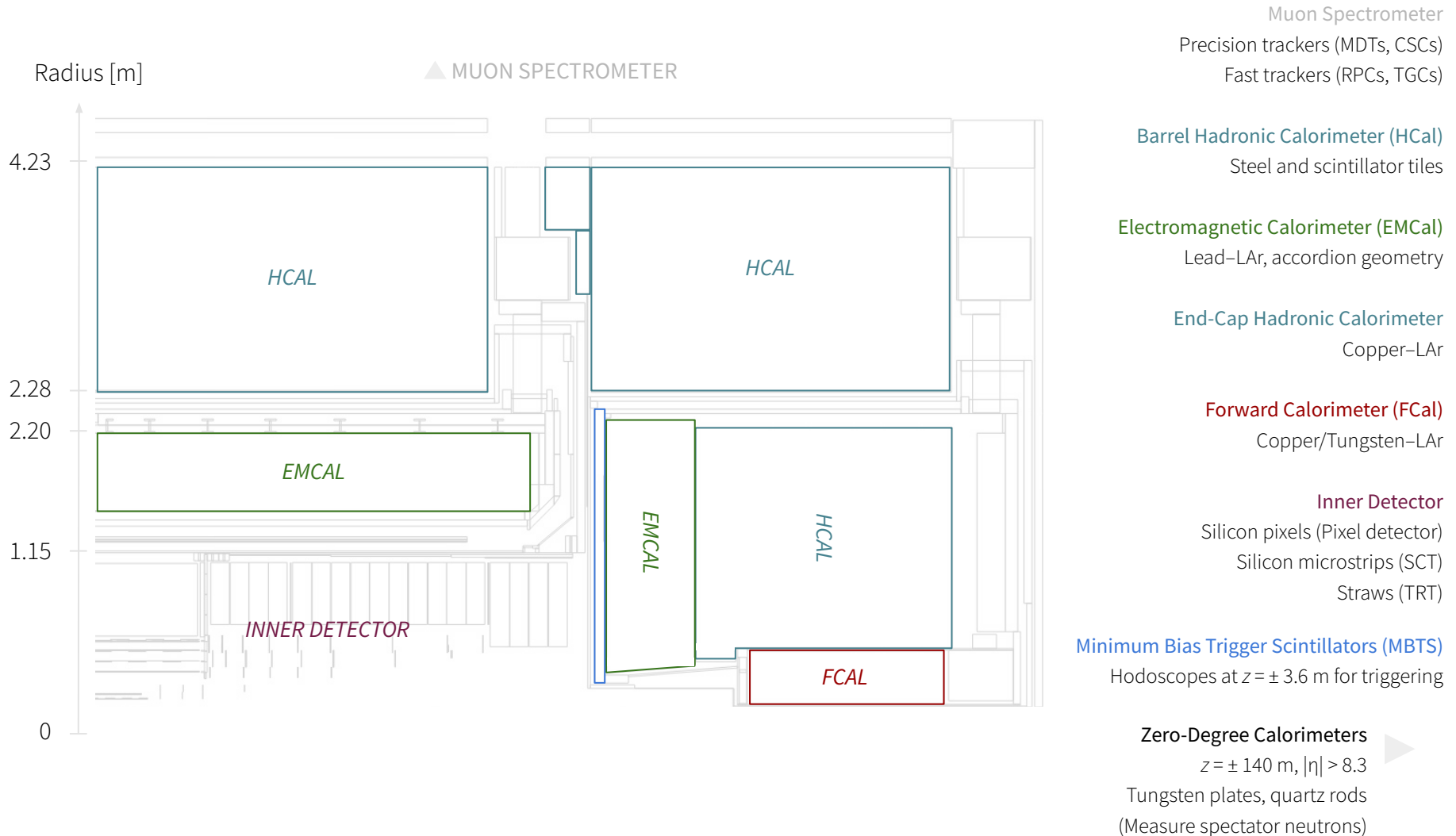


One of the first Heavy Ion collisions seen in ATLAS in November 2015

[\[More Event Displays\]](#)

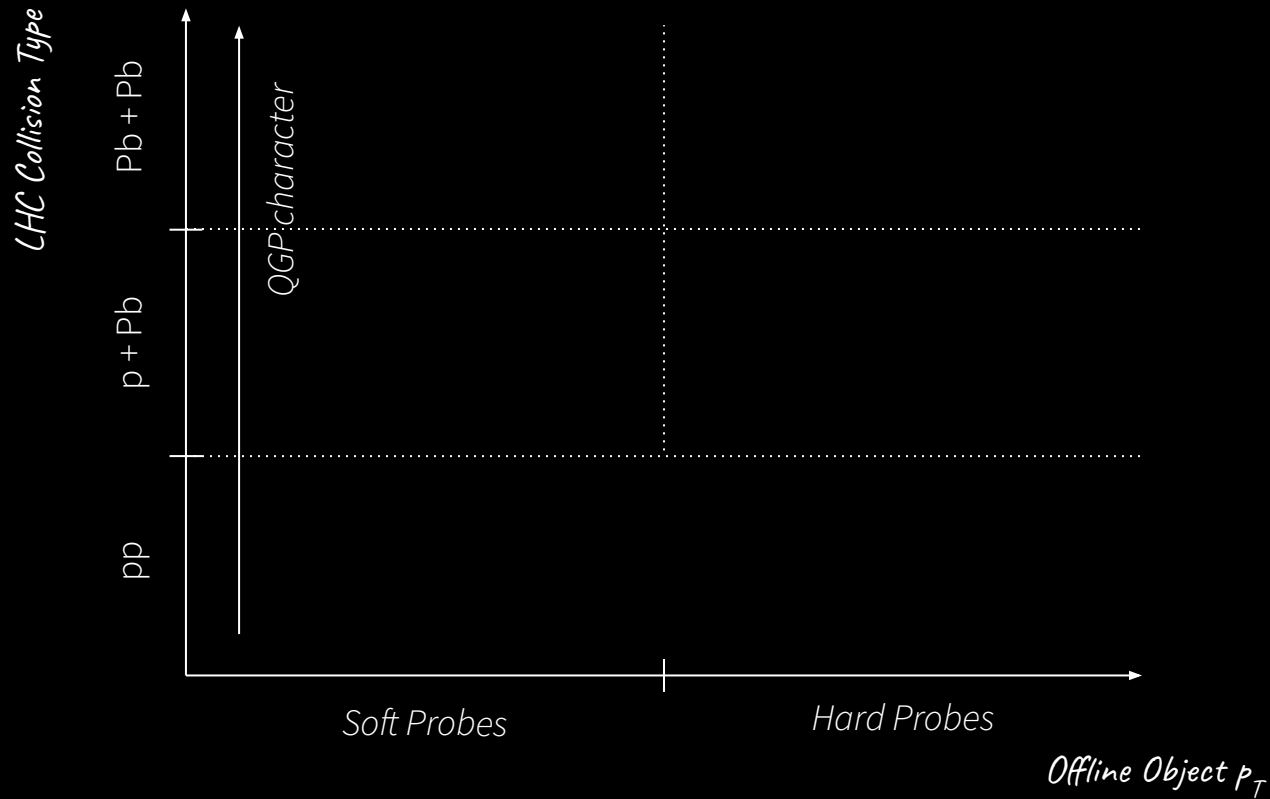
A Toroidal LHC Apparatus (ATLAS)

Designed to discover the Higgs boson



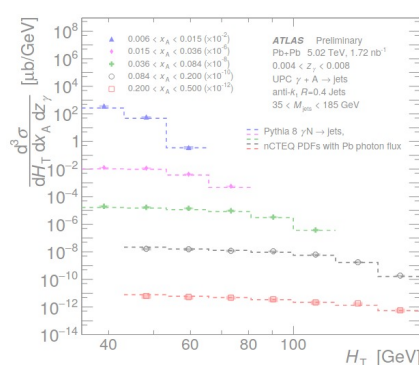
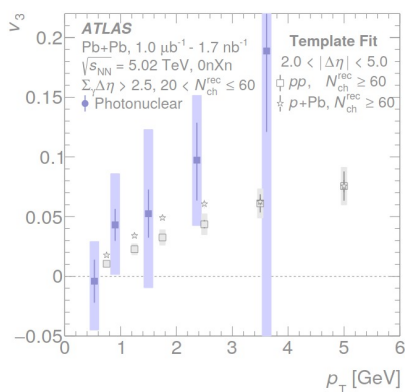
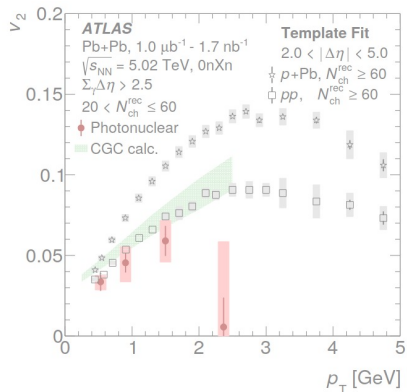
The Extreme QCD Programme of ATLAS

— Probes of the Quark Gluon Plasma (QGP) and precision tests of the Standard Model



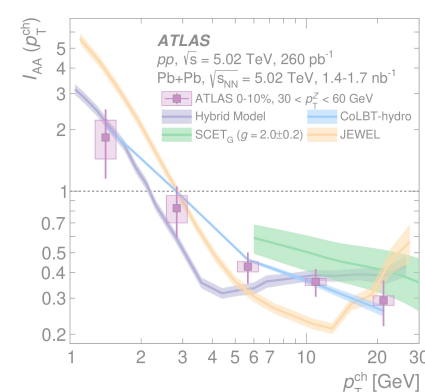
Today: A Cross-Section of Recent Results

8 extreme QCD results from the Heavy Ion and Standard Model groups



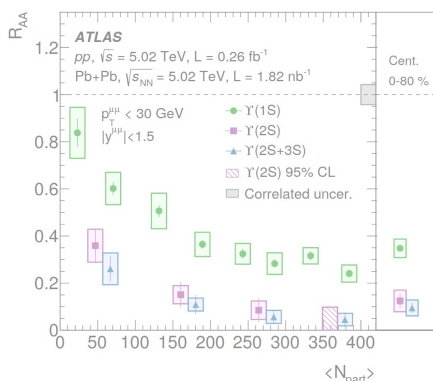
Flow Measurements [in Ultra-Peripheral Pb+Pb Collisions]

Two-Particle Azimuthal Correlations • Differential Dijet Cross-Sections



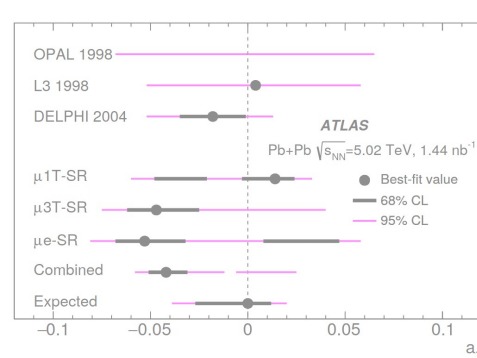
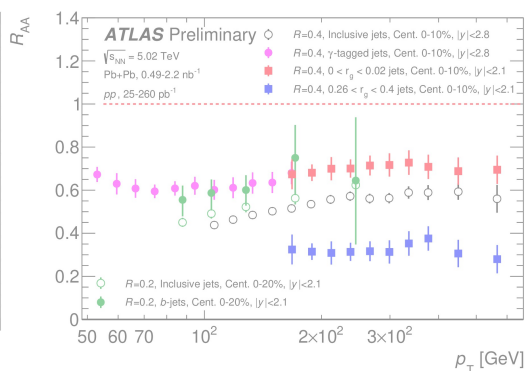
Hard Probes

Z Boson-Hadron Correlations



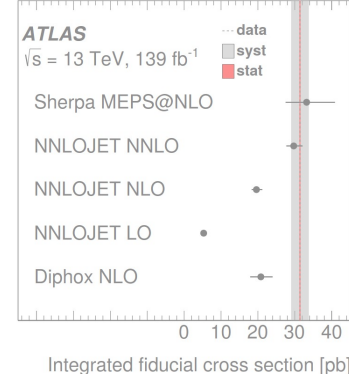
Hard Probes

$\Upsilon(nS)$ production • Summary of Jet Quenching • Jet Quenching in p+Pb



Precision Standard Model

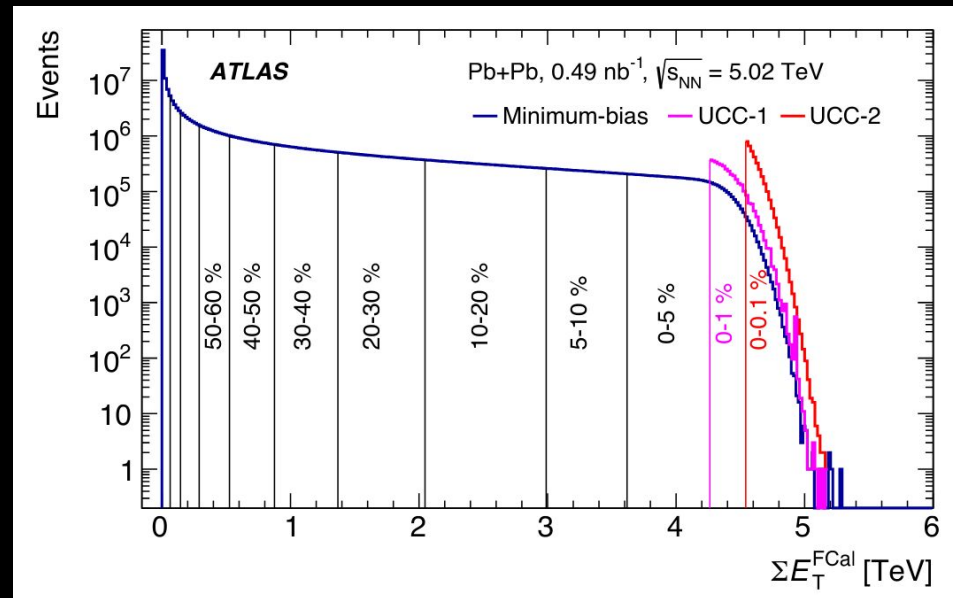
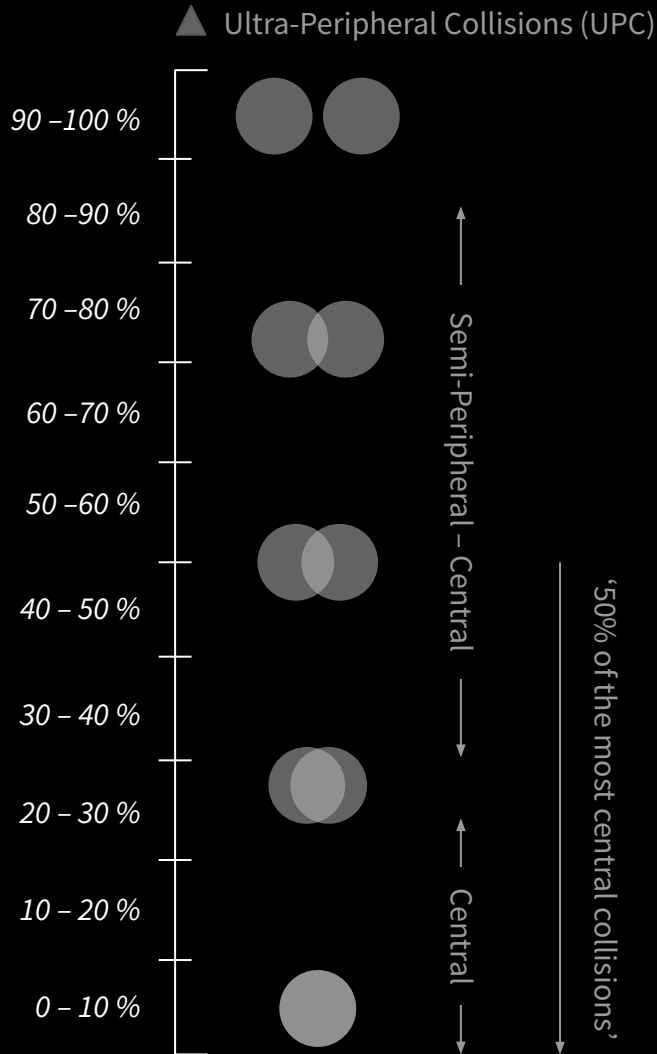
Observation of $\text{Pb}(\gamma\gamma \rightarrow \tau\tau)\text{Pb}$ • NNLO QCD Corrections



A non-exhaustive list — see all public results [here](#).

def. Centrality Intervals

A detector-level measure of nuclear overlap



UCC: Ultracentral Collisions trigger

UCC-1: total FCal $E_T > 4.21 \text{ TeV}$

UCC-2: total FCal $E_T > 4.54 \text{ TeV}$

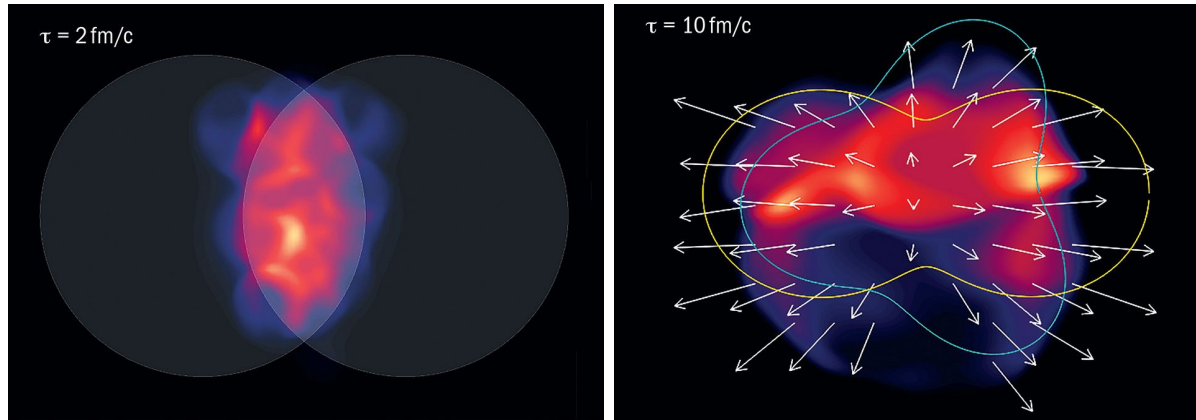
Strong monotonic correlation
with collision impact parameter

[Eur. Phys. J. C 78, 997 (2018)]

Two-Particle Azimuthal Correlations [PRC 104 (2021), 014903]

A classic measurement in Heavy Ion physics, for the first time in UPC

Initial-state non-uniformities ‘flow’ by rescattering into final-state momentum anisotropies parameterised as Fourier coefficients v_2 (ellipticity), v_3 (triangularity), up to fourth order



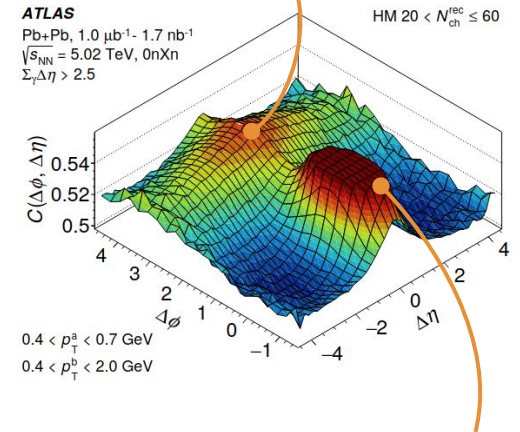
Collective behaviour is seen in large (Pb+Pb) and small (p+Pb, pp) systems

...but does it persist to even smaller systems like γ +Pb?

Measure v_2 and v_3 to find out

Away-side ridge $\Delta\phi \approx \pi$

Due to momentum conservation
(a *non-flow* contribution)



Near-side peak $(\Delta\phi, \Delta\eta) \approx (0, 0)$

From correlations between jet fragments
(non-flow and truncated to show other structures)

Footnote: the exact parameterisation

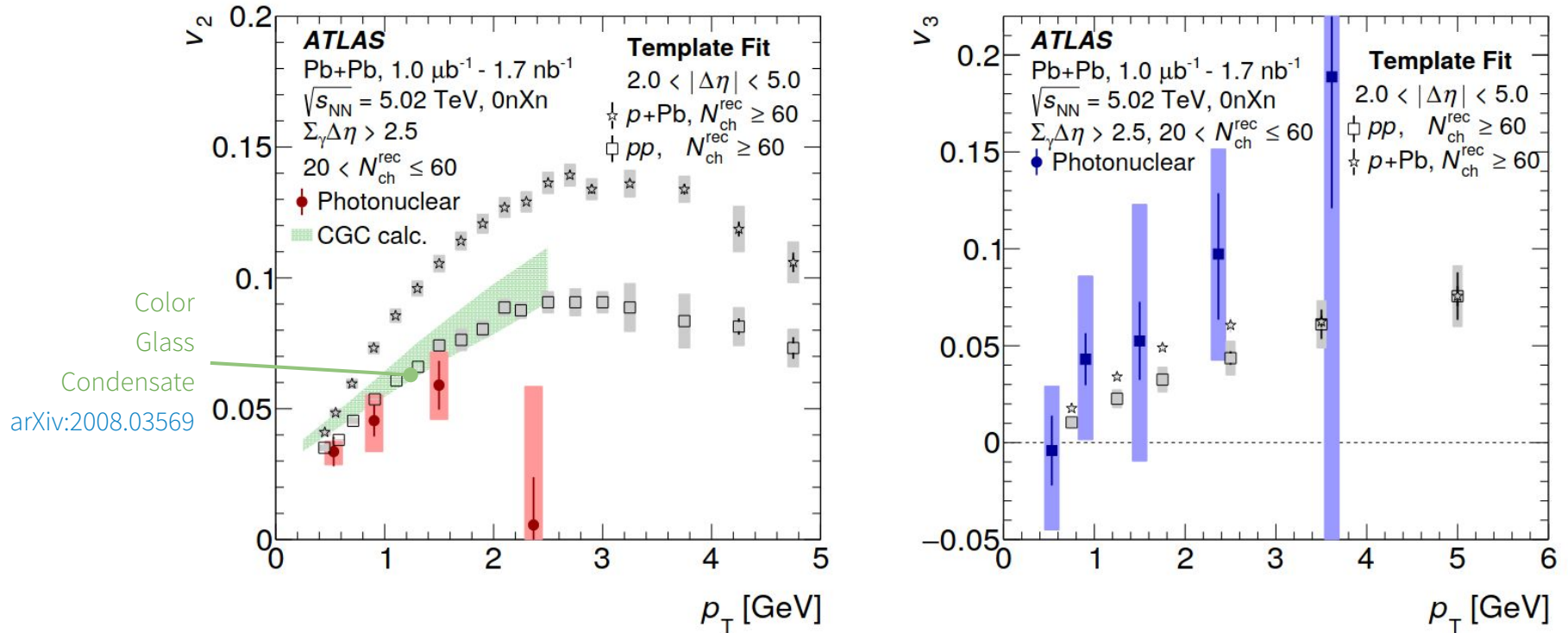
Sum of an azimuthally-modulated pedestal function and a non-flow component templated from Low Multiplicity (LM) events

$$Y^{\text{HM}}(\Delta\phi) = FY^{\text{LM}}(\Delta\phi) + G \left\{ 1 + 2 \sum_{n=2}^4 v_{n,n} \cos(n\Delta\phi) \right\}$$

Two-Particle Azimuthal Correlations [PRC 104 (2021), 014903]

Observation of non-zero flow parameters v_2 and v_3

Measurement performed in 2018 Minimum-Bias and High-Multiplicity photonuclear events with rapidity gaps, assuming factorisation of the two-particle flow coefficients into single-particle coefficients



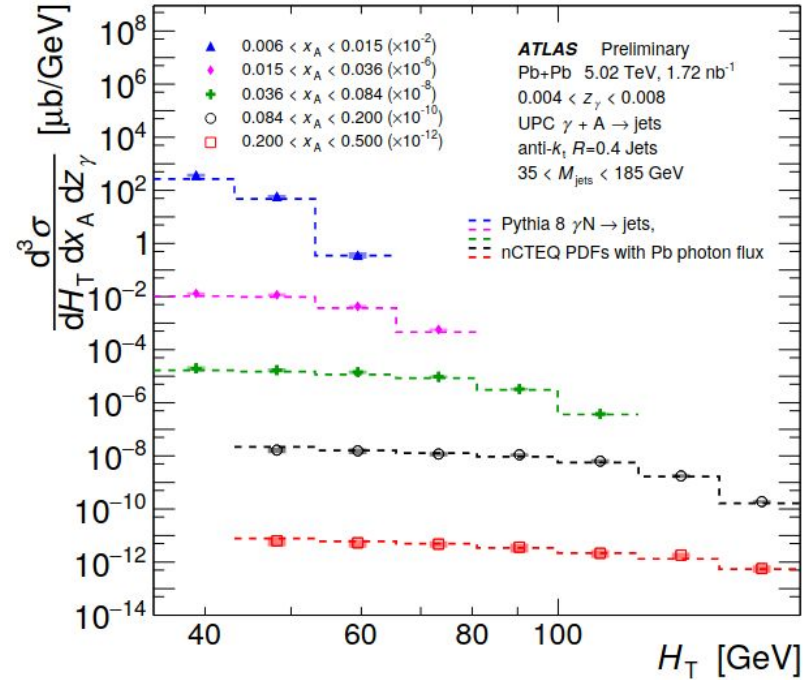
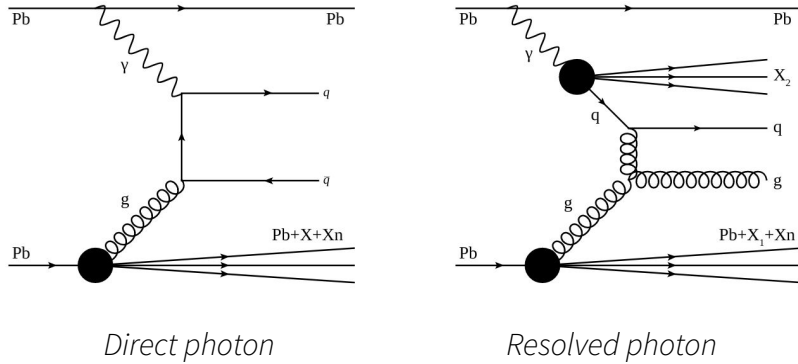
First observation of significant non-zero flow coefficients in UPC

Caveat: factorisation only demonstrated in v_2 in $0.4 < p_{\text{T}} < 2 \text{ GeV}$ — violation at high p_{T} (negative $v_n \dots$)?

Otherwise, consistency with other collision systems (within large uncertainties)

Towards precise limits on nuclear PDFs

Leading-order contributions to dijet production in UPC



Fiducial phase space

$$p_T^{\text{jet}} > 15 \text{ GeV}$$

$$|\eta^{\text{jet}}| < 4.4$$

0nXn ZDC signature

Sum-of-gaps > 2.5

Pb-going edge gap < 3

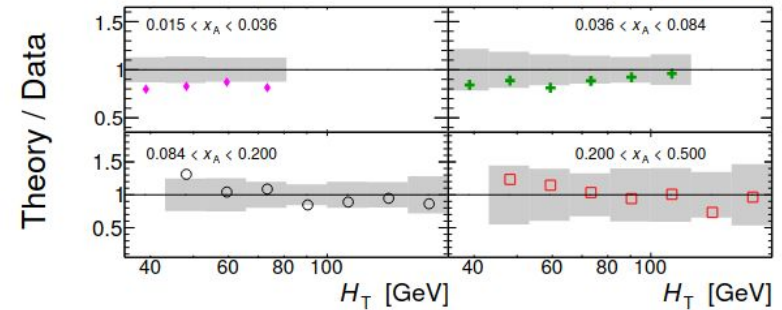
$$H_T \equiv \sum_i p_{T,i}$$

$$z_\gamma \equiv \frac{M_{\text{jets}}}{\sqrt{s_{\text{NN}}}} e^{+y_{\text{jets}}}$$

$$x_A \equiv \frac{M_{\text{jets}}}{\sqrt{s_{\text{NN}}}} e^{-y_{\text{jets}}}$$

UNFOLD*

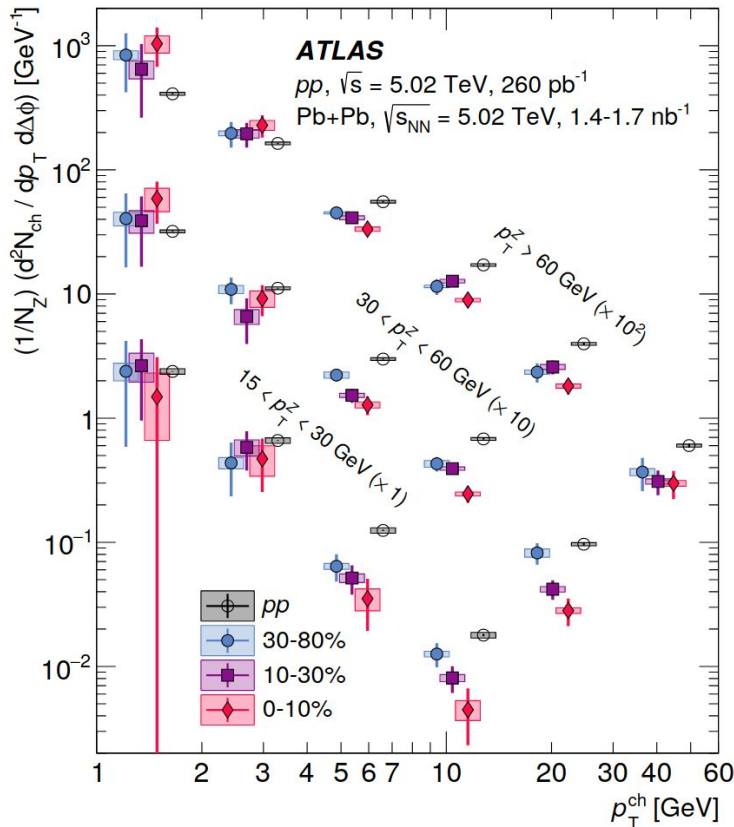
*Total jet transverse momentum and beam momentum fractions



Pb+Pb medium-induced modifications to Z-tagged charged-particle yields

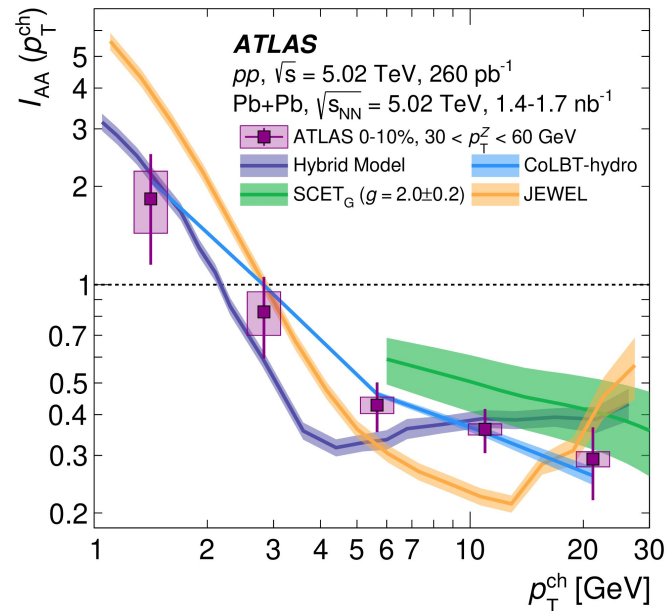
Z boson does not interact with the QGP

Use it to deduce the initial kinematics of the hard-scattered partons in Z+jet events without bias



Charged-particle yield per Z boson

Yield suppression in data vs models



Hybrid Model

Pythia 8 + energy loss from holographic methods

CoLBT-hydro

Boltzmann transport and hydrodynamics model

SCET_G

Perturbative calculation with a jet-medium coupling

JEWEL

QCD jet with radiative and elastic energy loss

Systematic modification of the per-Z yields in Pb+Pb collisions

Due to interactions between the QGP and parton shower — *but what is the mechanism of energy loss?*

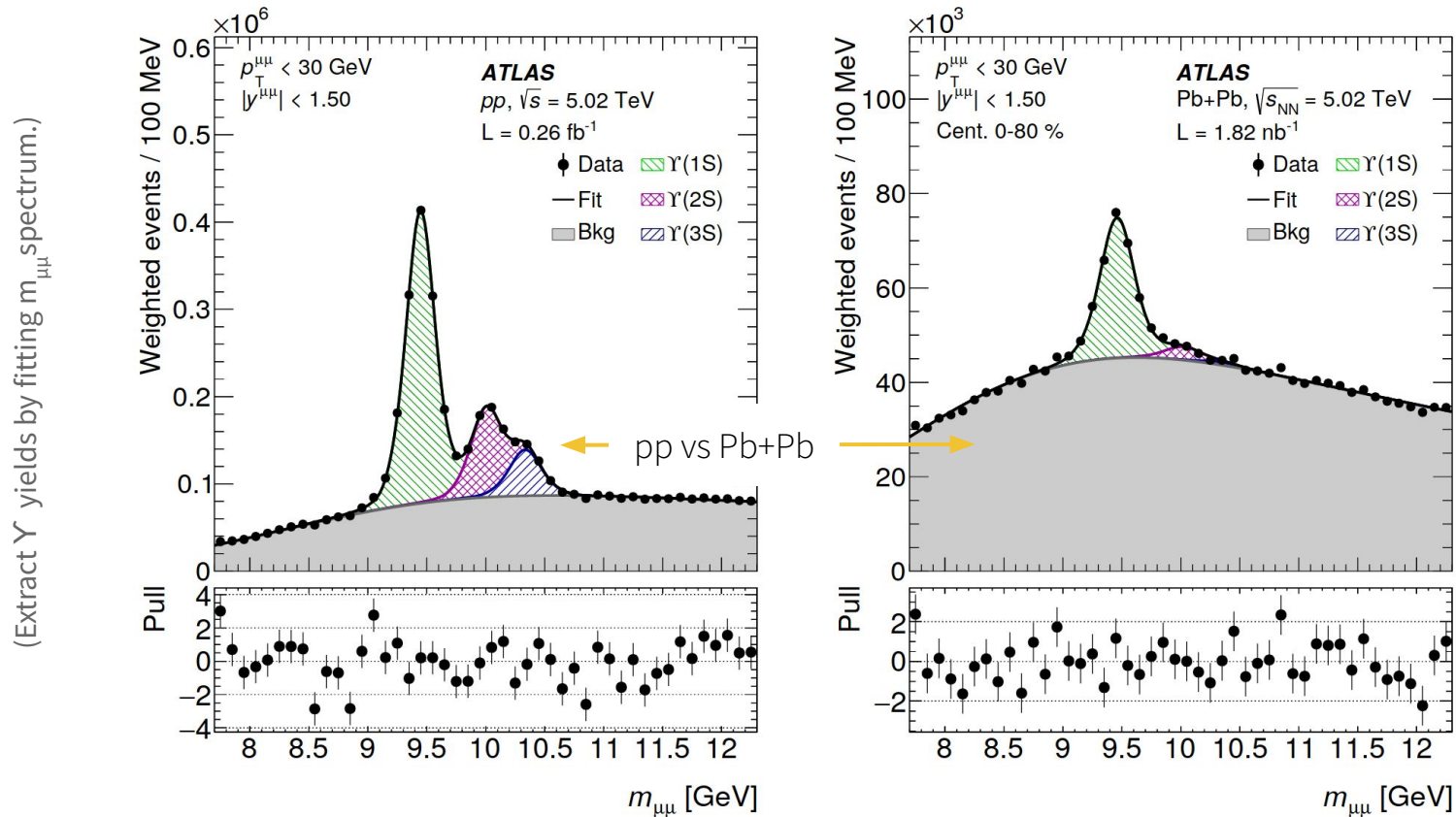
$\Upsilon(nS)$ production

[(Submitted to PRC)]

Footage of the Quark Gluon Plasma in Pb+Pb collisions

Measurement in the dimuon decay channel, in fiducial phase space

$p_T^{\mu\mu} < 30$ GeV and absolute rapidity $|y^{\mu\mu}| < 1.5$ and centrality 0–80%



Bottom quarks are produced early in the formation of the Quark Gluon Plasma

— and can be used to probe its full evolution

$\Upsilon(nS)$ production

[(Submitted to PRC)]

Suppression of Pb+Pb vs pp and $\Upsilon(nS)$ vs $\Upsilon(1S)$

$$R_{AA} = \frac{N_{AA}}{\langle T_{AA} \rangle \times \sigma_{PP}}$$

Per-event Υ yields in Pb+Pb

pp cross-section at same \sqrt{s}

Mean nuclear overlap (from MC)

Nuclear modification factor

Suppression of all states across entire range of centrality

No $p_T^{\mu\mu}$ or $y^{\mu\mu}$ dependence

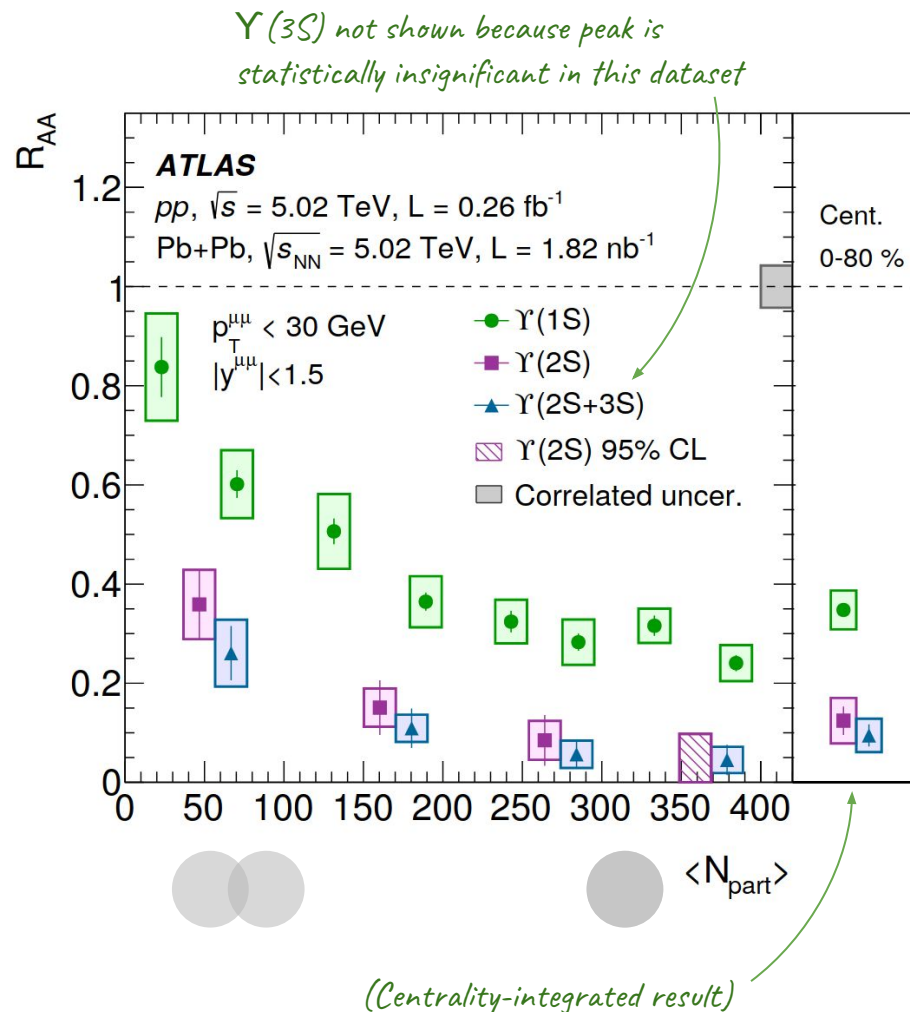
$\Upsilon(2S)$ and $\Upsilon(2S+3S)$ more suppressed

$$\rho_{AA}^{\Upsilon(nS)/\Upsilon(1S)} = R_{AA}(\Upsilon(nS))/R_{AA}(\Upsilon(1S))$$

Excited-to-ground state double ratios

All smaller than one – sequential suppression

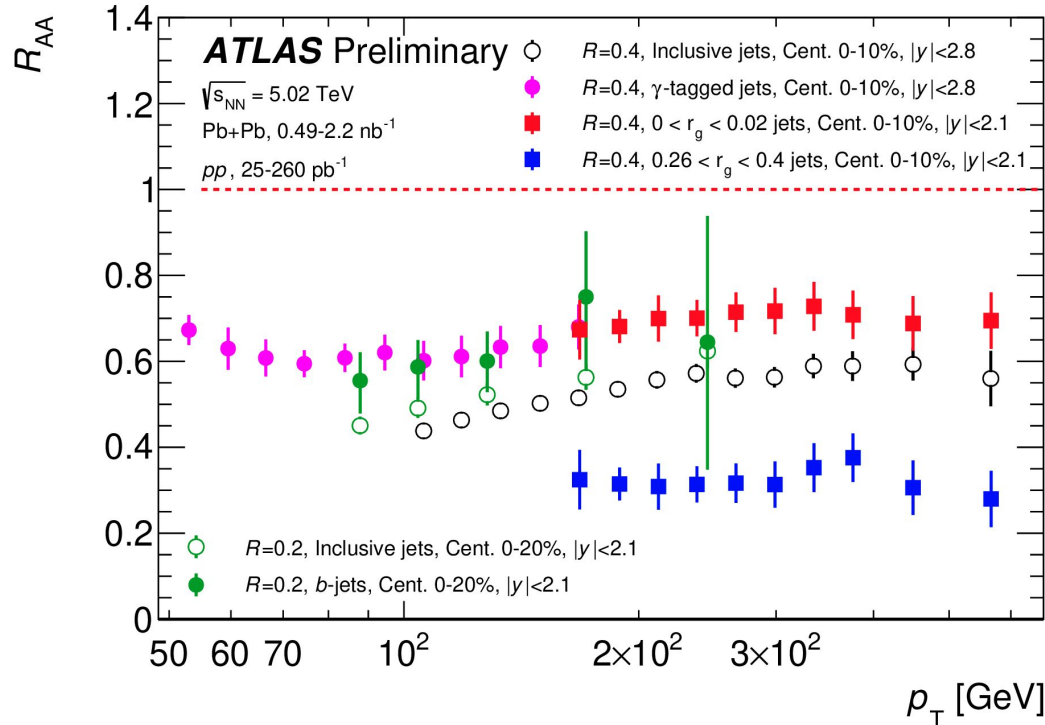
Compared to various predictions...



Summary of Jet Quenching Measurements

Mass matters – but it isn't the only thing

(For completeness [[Heavy Ion Summary \$R_{AA}\$ plots, 2022](#)])



○ Inclusive jets

Decrease of quenching with increasing p_T
Increase towards peripheral collisions
[PLB 790 \(2019\) 108](#)

● γ -tagged jets

Photon triggers — access lower jet p_T
Dominantly quark-initiated — less quenching by radiative emission models
[ATLAS-CONF-2022-019](#)

■ ■ Substructure-dependent jets

r_g : angular scale of the first hard splitting
Results consistent with coherence quenching
[ATLAS-CONF-2022-026](#)

○ ● $R = 0.2$ inclusive vs b -jets

Heavy jets less suppressed than inclusive jets
Suggests a role for mass and colour in energy loss
[\(Submitted to EPJC\)](#)

○ □ Also: dijets

Increased fraction of imbalanced jets compared to in pp
Subleading jets significantly more suppressed
[\(Submitted to PRC\)](#)

Jet Quenching

[(Submitted to PRL)]

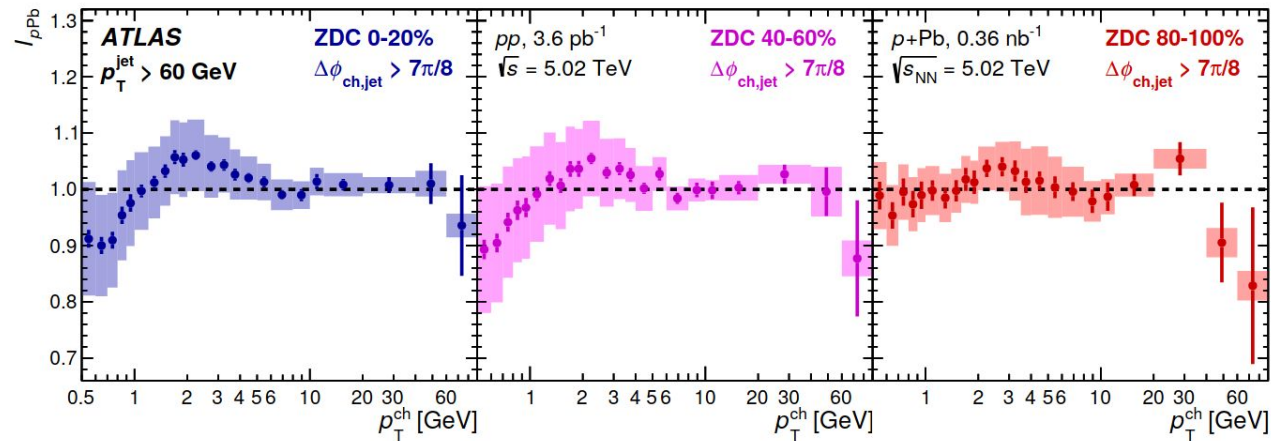
Or a lack thereof (?) in p+Pb collisions

Jet quenching ~ the process of color-charged partons losing energy via interactions with the QGP

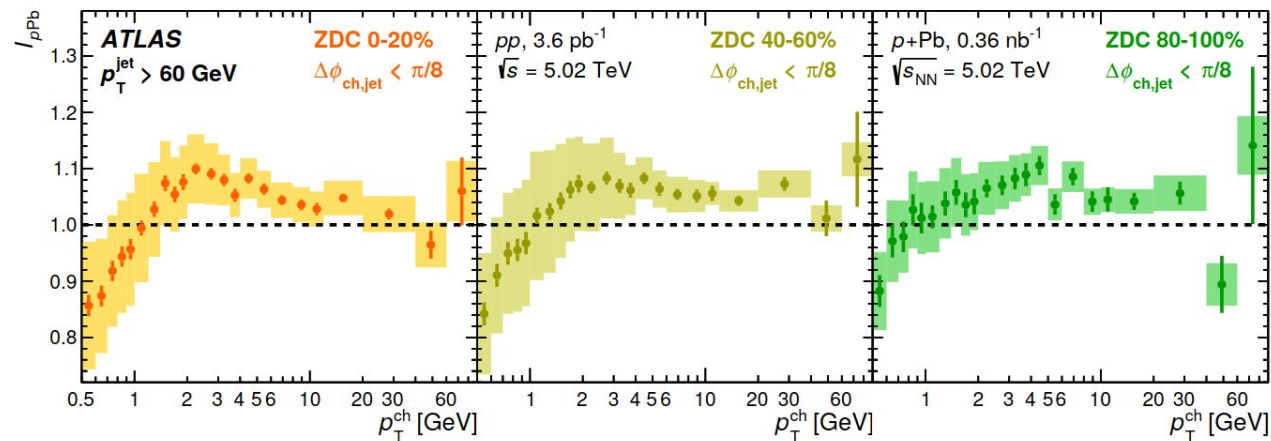
Collectivity is seen in smaller systems, but does jet quenching also occur in p+Pb?

$$I_{pPb} = Y_{pPb}/Y_{pp}$$

Away-side.



Near-side.



Centrality \longrightarrow

\Rightarrow Severe constraint on the amount of jet quenching in p+Pb collisions

Latest in Photon-Fusion

The observation of $Pb(\gamma\gamma \rightarrow \tau\tau)Pb$

[(Submitted to PRL)]

$\gamma\gamma \rightarrow \tau\tau$

Apr 2022

[arXiv:2204.13478](https://arxiv.org/abs/2204.13478)

$\gamma\gamma \rightarrow ee$

Apr 2022

[ATLAS-CONF-2022-025](https://arxiv.org/abs/2204.025)

$\gamma\gamma \rightarrow \gamma\gamma$

Jul 2019

[JHEP 03 \(2021\) 243](https://arxiv.org/abs/1907.0243)

[PRL 123 \(2019\), 052001](https://arxiv.org/abs/1905.02001)

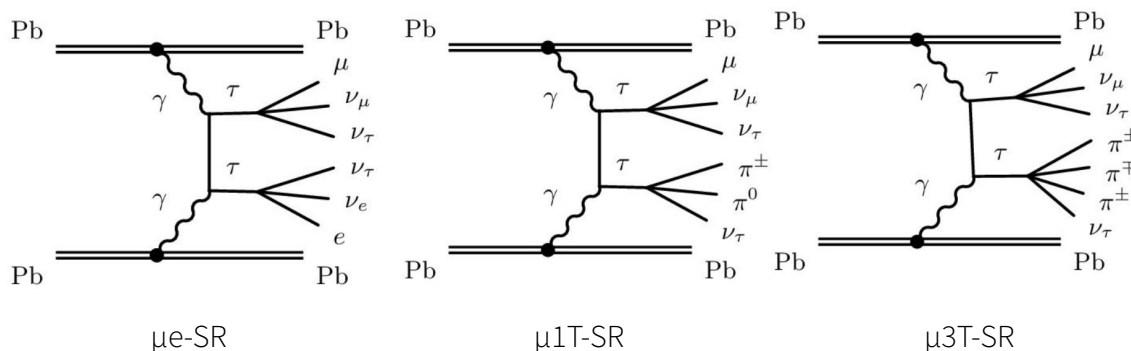
[Nat. Phys. 13, 852-858 \(2017\)](https://arxiv.org/abs/1708.0852)

$\gamma\gamma \rightarrow \mu\mu$

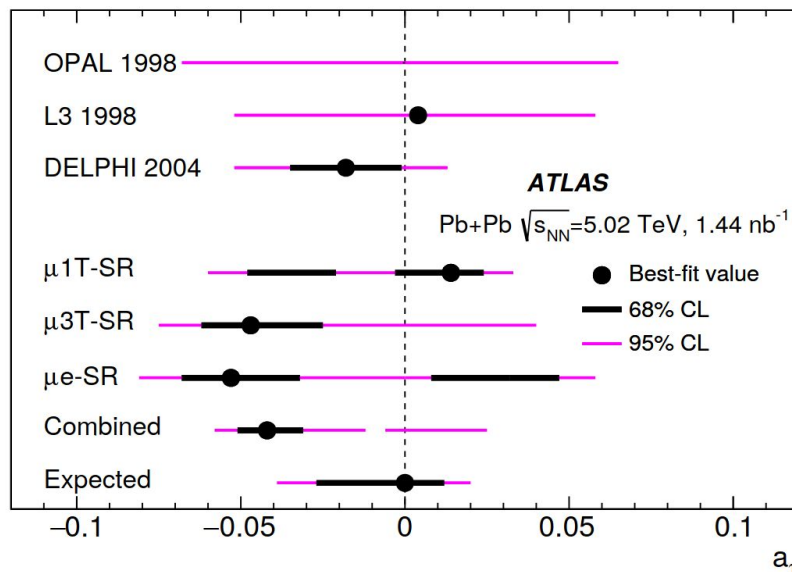
Nov 2018

[PRL 121 \(2018\), 212301](https://arxiv.org/abs/1811.21230)

[PRC 104 \(2021\), 024906](https://arxiv.org/abs/2102.04906)



Profile-likelihood fits



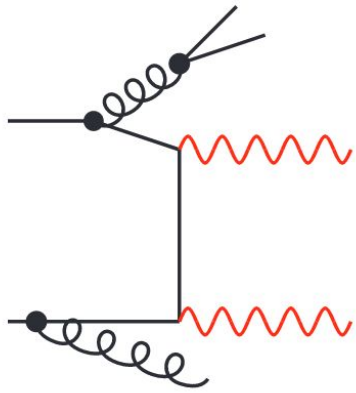
Signal strength:

$$\mu_{\tau\tau} = 1.04^{+0.06}_{-0.05} \text{ (tot)}$$

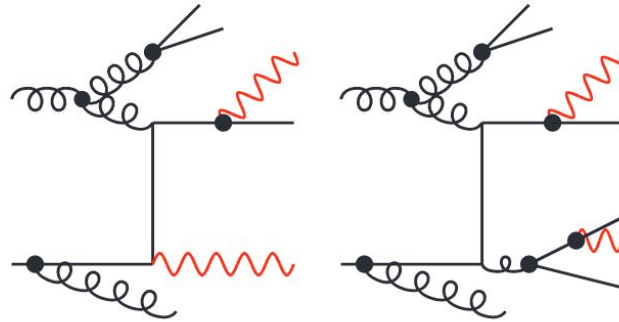
Constraints on the tau lepton's anomalous magnetic moment,

$$a_\tau = (g_\tau - 2)/2$$

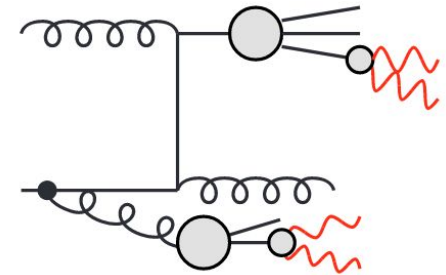
Prompt production of photon pairs in 13 TeV pp collisions



Direct



Single and double fragmentation



Non-prompt and misidentification



NNLOJET

Fixed-order NNLO (antenna-subtraction method; NNPDF3.0NNLO)



DIPHOX

Fixed-order NLO (CT10 NLO)

SHERPA 2.2

Fixed-order NLO with MEPS@NLO
($pp \rightarrow \gamma\gamma + 0,1j$ at NLO; $pp \rightarrow \gamma\gamma + 2,3j$ at LO; NNPDF3.0NNLO)



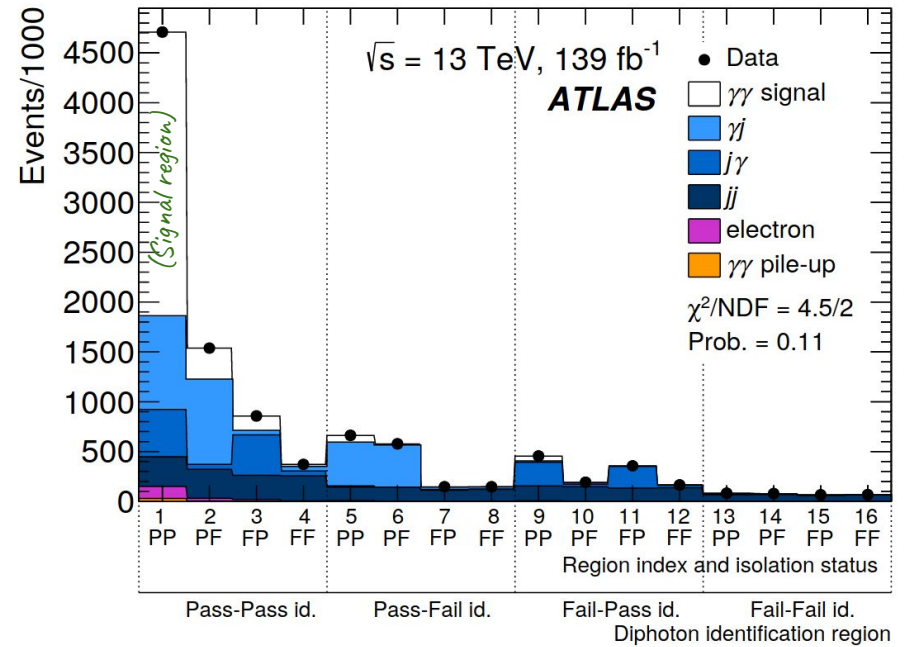
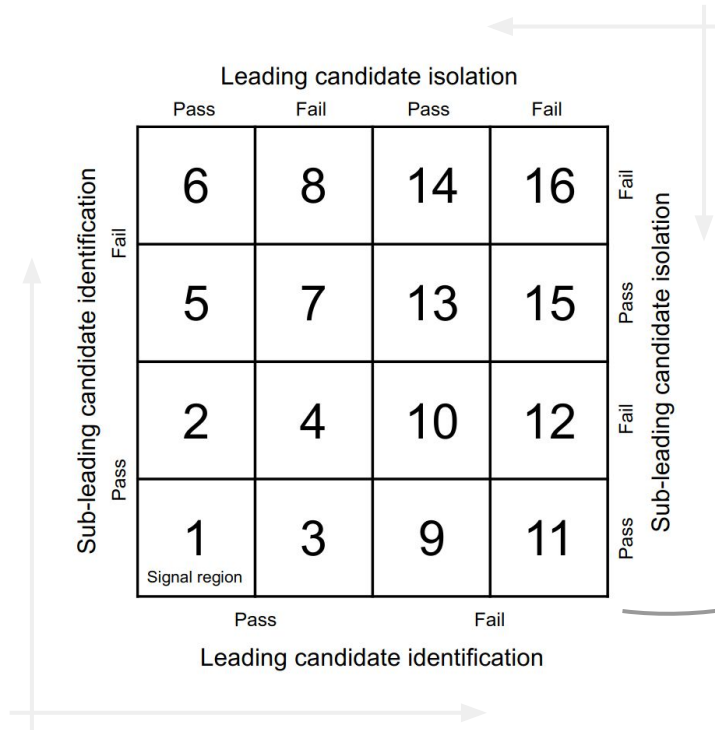
DATA

Estimation of the $\{\gamma\gamma, j\gamma, jj, ee, \text{pileup}\}$ backgrounds

2x2D side-bands method

[A technique from diphoton analyses]

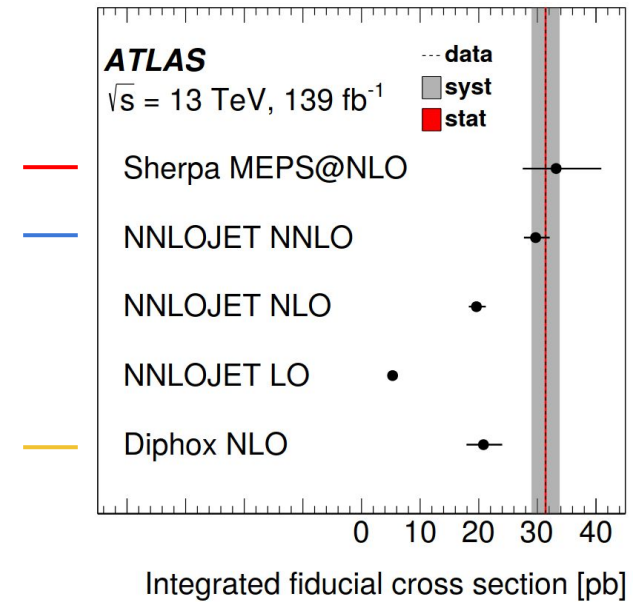
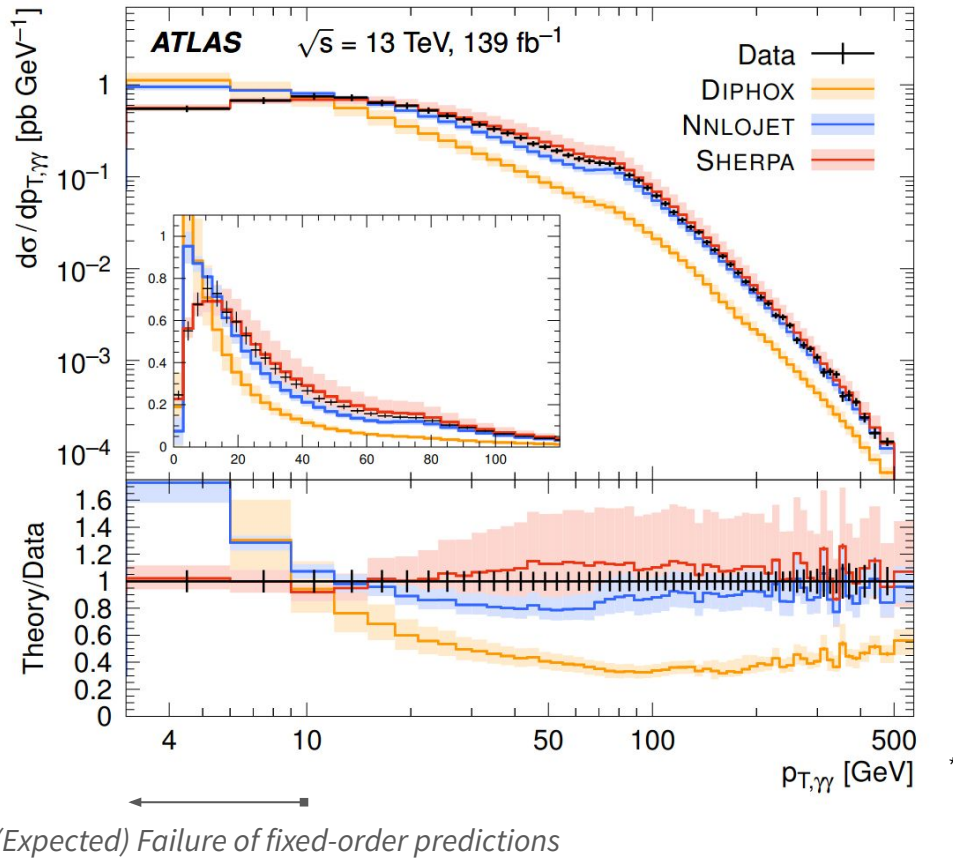
- Define 15 background-enriched control regions
- Extrapolate using a profile likelihood fit



Unfolding to particle-level

Using an iterative technique based on Bayes' theorem.
To compare with theory predictions without detector effects.

Results: differential and integrated cross-sections

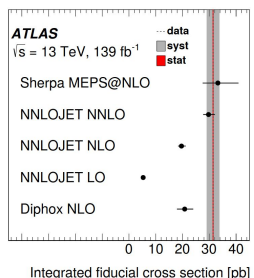
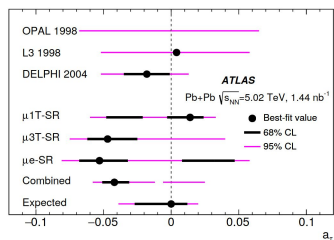
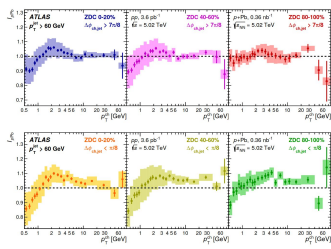
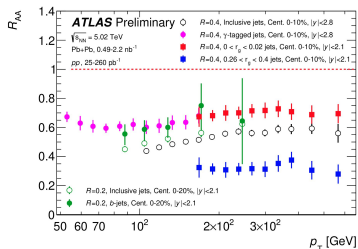
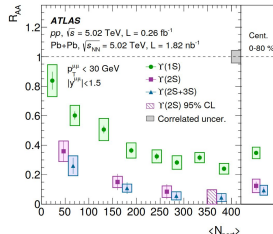
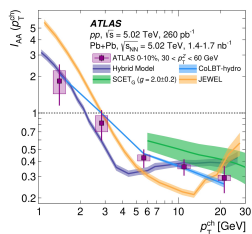
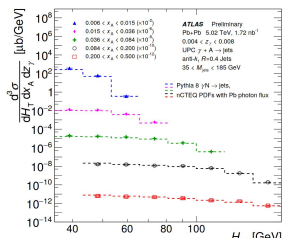
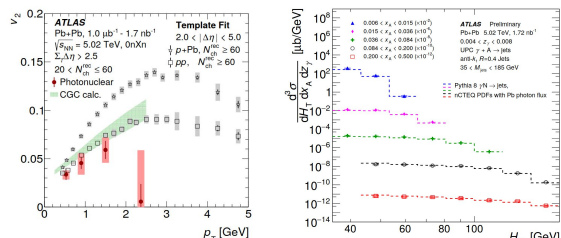


Fiducial cross section [pb]	$\sigma_{\gamma\gamma}$	$\pm \text{unc.}$
SHERPA MEPS@NLO	33.2	+7.7 -5.6
NNLOJET NNLO	29.7	+2.4 -2.0
NLO	19.6	+1.6 -1.3
LO	5.3	+0.5 -0.5
DIPHOX NLO	20.8	+3.2 -2.9
Data	31.4	2.4

* (Also $p_{T,\gamma}, m_{\gamma\gamma}, |\cos \theta^*|^{(\text{CS})}$ (scattering angle in Collins–Soper frame), ϕ_η^* , $\pi - \Delta\phi_{\gamma\gamma}$ (acoplanarity), $a_{T,\gamma\gamma}$ (p_T transverse to thrust axis))

Summary

8 extreme QCD results



1. Two-Particle Azimuthal Correlations

Non-zero v_2 and v_3 flow coefficients observed in p+Pb

2. Differential Cross-Sections of Dijet Production in UPC

An important step towards precise limits on nuclear PDFs

3. Z Boson-Hadron Correlations in Pb+Pb

Systematic quenching of the shower

4. Suppression of Y(nS) States in Pb+Pb Collisions

5. Summary of Jet Quenching Measurements

6. Strong Constraints on Jet Quenching in p+Pb

7. Observation of Photon-Fusion to τ -Lepton Pairs

With interpretation of the τ -lepton's anomalous magnetic moment

8. Verification of NNLO Predictions in γ -Pair Production Data

And more to come from ATLAS in Run 3 and beyond

BACKUP

Schematic of the Liquid Argon (LAr) Calorimeter

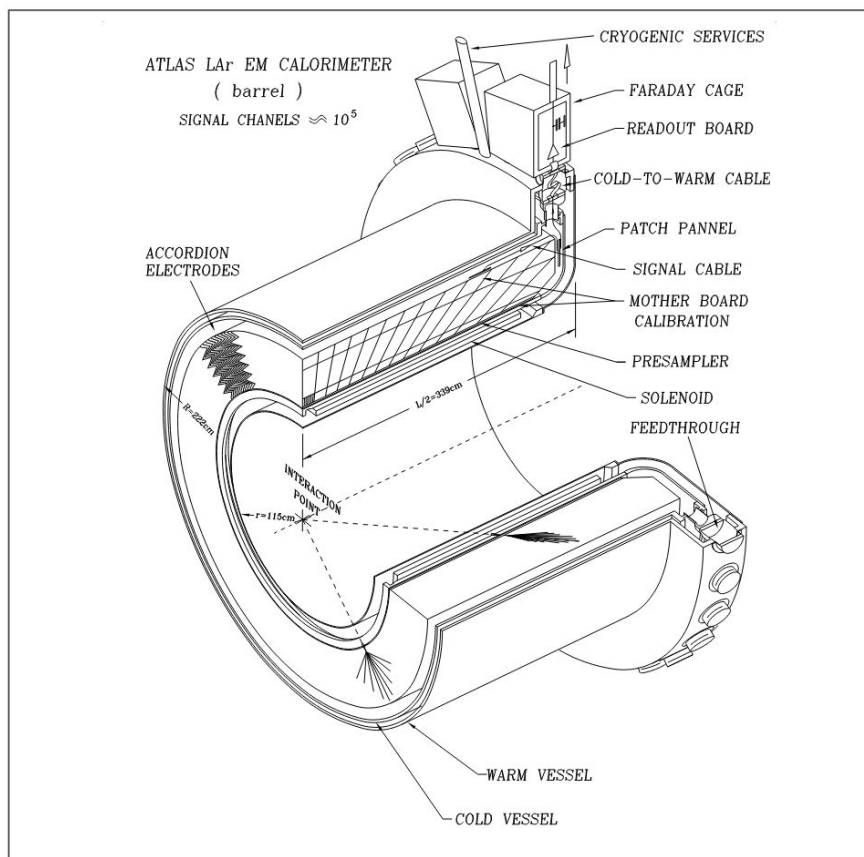


Figure 1-1 Perspective view of one half of the barrel cryostat.

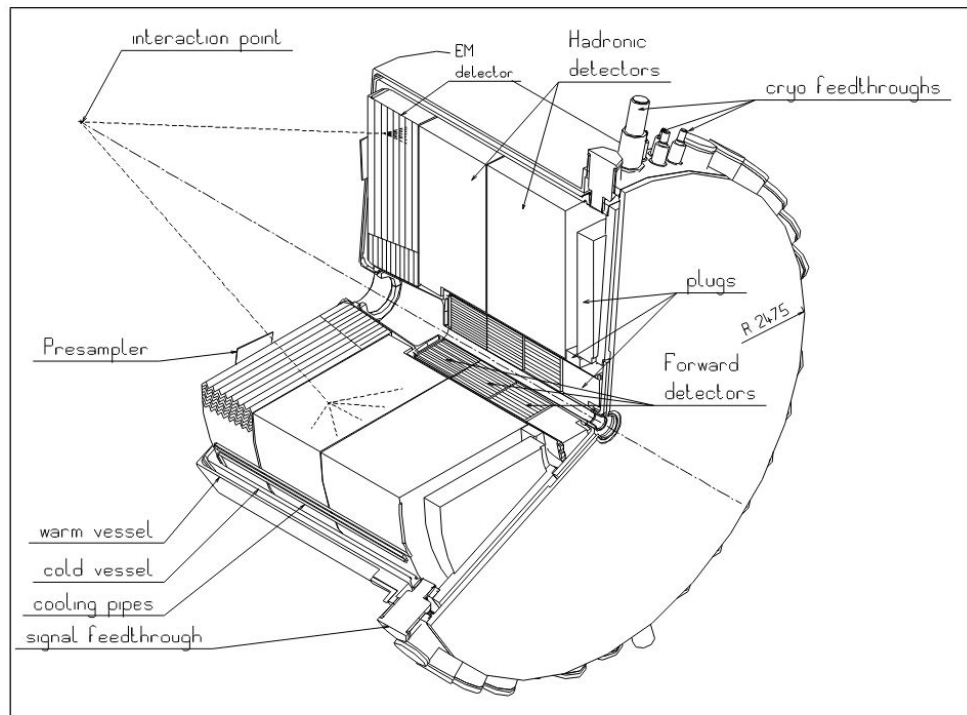
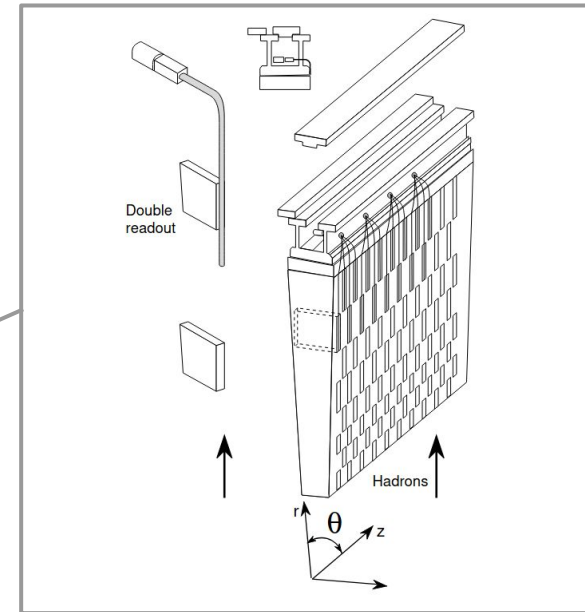
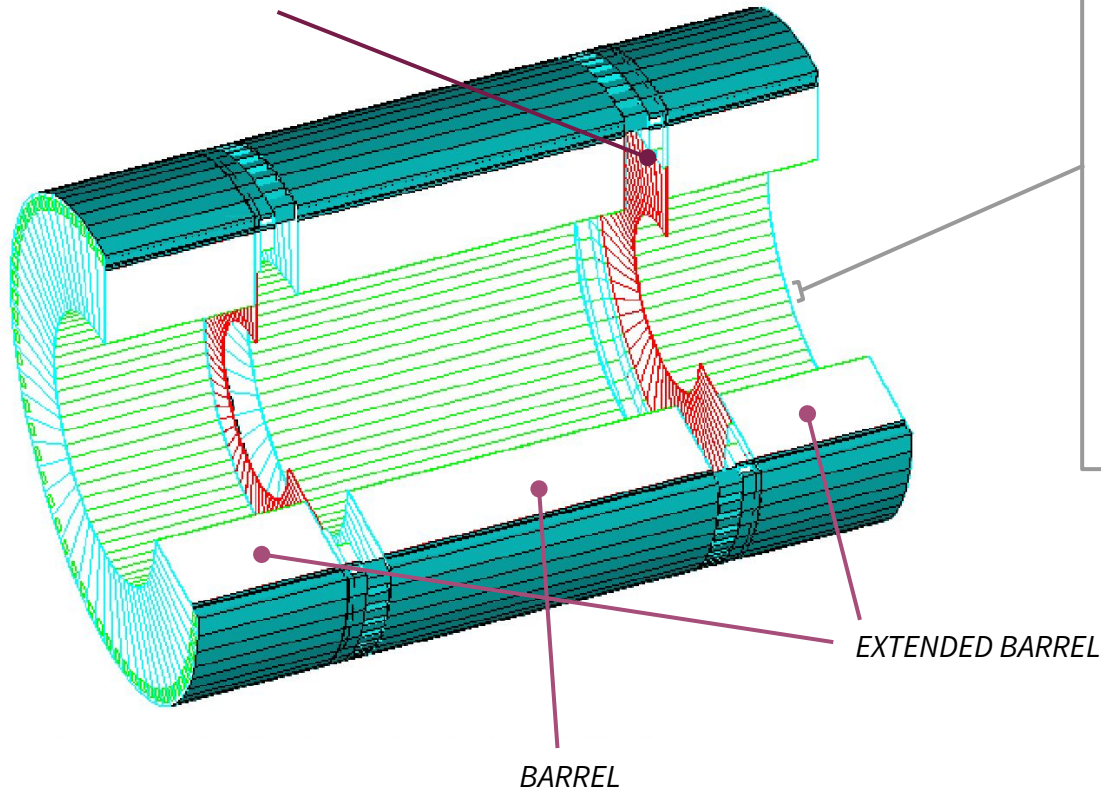


Figure 1-3 Perspective view of one end-cap cryostat.

Technical Design Report of the LAr Calorimeter, [CERN-LHCC-96-041](#)

Schematic of the Tile Calorimeter

Plug calorimeter, and gap and crack scintillators forming the *INTERMEDIATE TILE CALORIMETER*



Technical Design Report of the Tile Calorimeter, [CERN-LHCC-96-042](#)

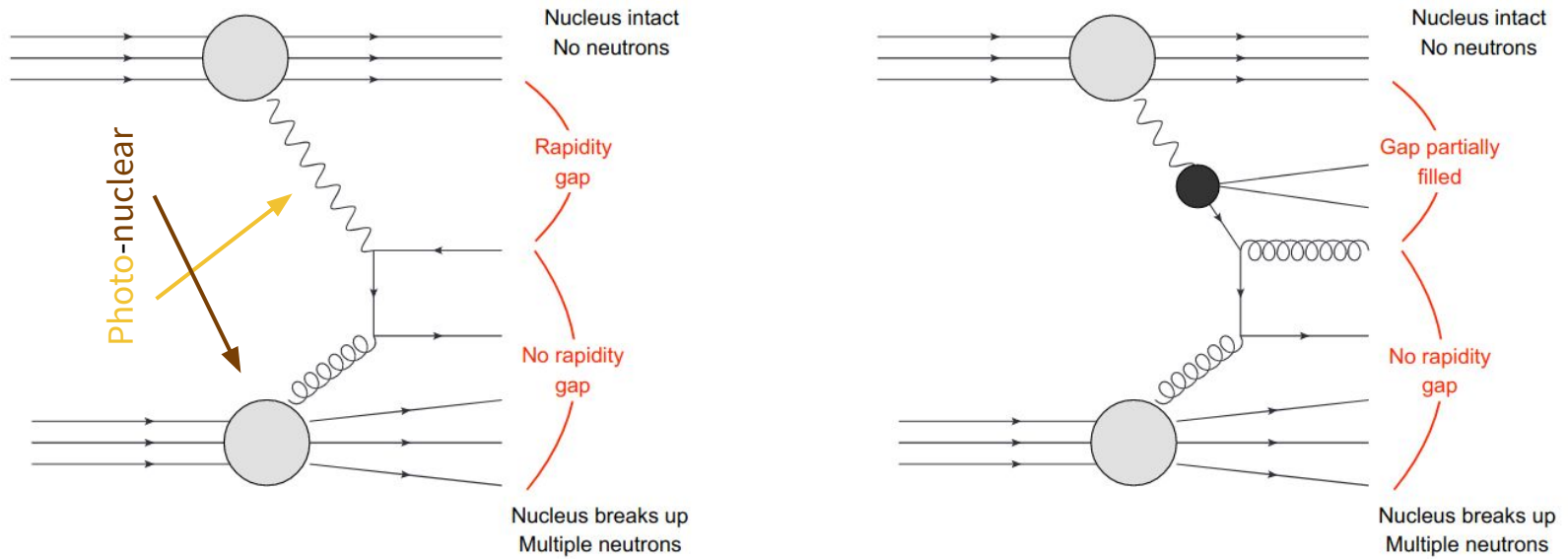
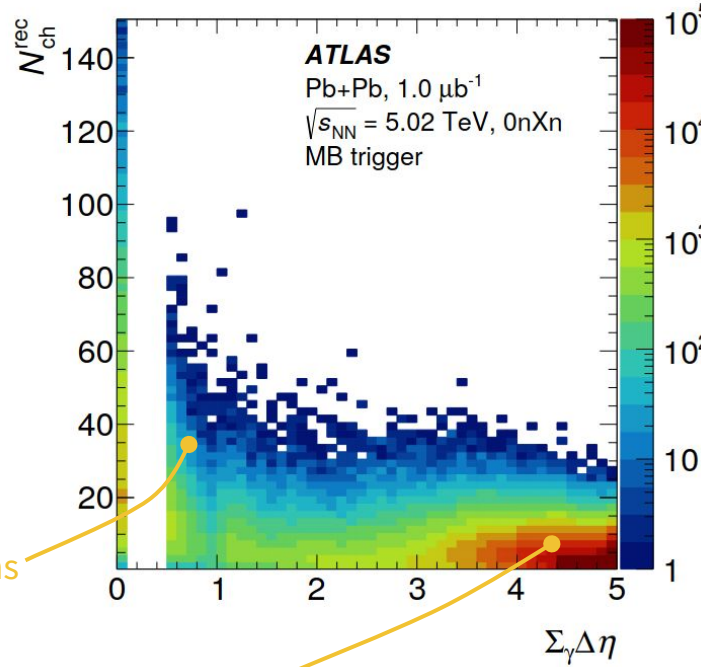


Figure 1: Diagrams representing different types of photonuclear collisions and the general features of their event topologies. *Left:* the direct process, in which the photon itself interacts with the nucleus. *Right:* the resolved process, in which the photon fluctuates into a hadronic state.

[From ATLAS, *Two-Particle Azimuthal Correlations in Photonuclear Ultrapерipheral Collisions*, Jul 2021, [2101.10771](https://arxiv.org/abs/2101.10771)]

'Sum of Gaps' Rapidity Gap

[2101.10771]

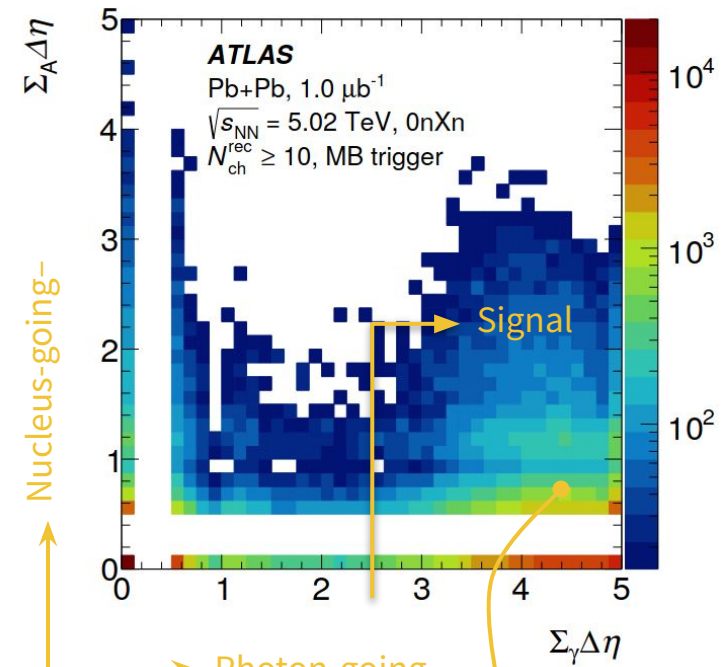


Hadronic Pb+Pb collisions

Broad $N_{\text{ch}}^{\text{rec}}$ distribution.
Small sum of gaps.

Photon-induced collisions

Large sums-of-gaps.
Steep $N_{\text{ch}}^{\text{rec}}$ distribution.



Nucleus-going-

Photon-going-

Photon-induced collisions

Large photon-going sums-of-gaps.
Small nucleus-going sum-of-gaps.

Sum of gaps algorithm: (i) sort tracks and calorimeter clusters in η , (ii) add together contiguous rapidity gaps that are greater than $\Delta \eta = 0.5$ (so that gaps may be separated by isolated slivers of particle production). This captures *resolved* photonuclear collisions in addition to direct photonuclear collisions.

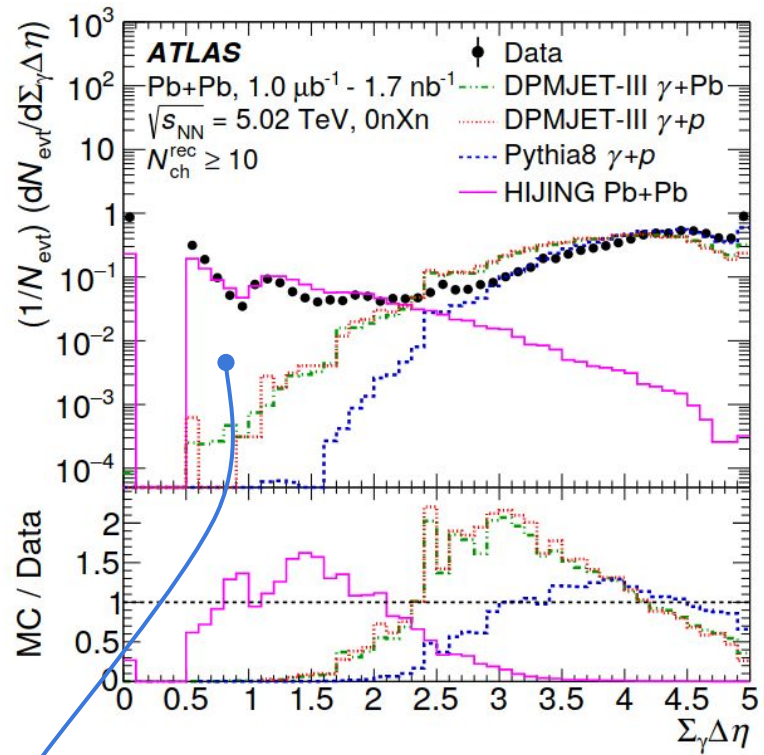
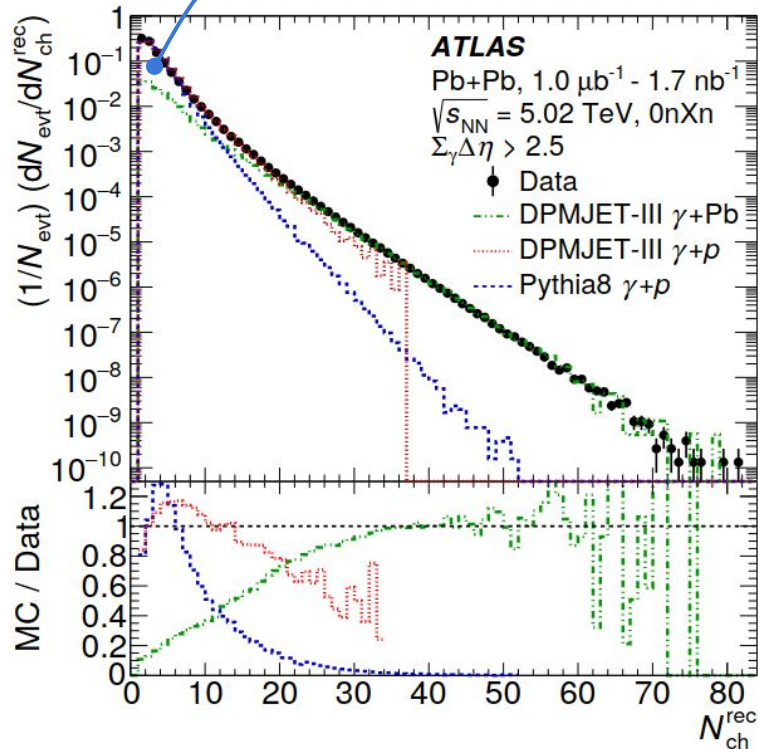
p+Pb Modelling Performance

[2101.10771]

DPMJET-III γ +Pb vs γ +p vs Pythia 8 γ +p

Non-photonuclear processes, or poor modelling?

Poor DPMJET-III performance at $N < 15$



Residual peripheral Pb+Pb

Two-Particle Correlations $C(\Delta\phi, \Delta\eta)$

[2101.10771]

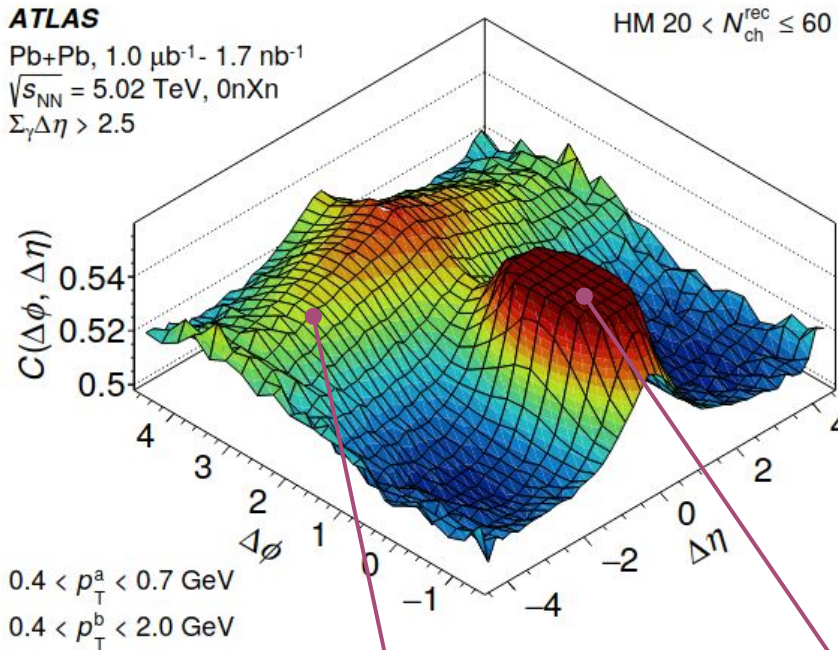
Emphasis on the near-side peak and away-side ridge

$$C(\Delta\phi, \Delta\eta) = \frac{1}{N_a} \frac{d^2 N_{\text{pair}}}{d\Delta\phi d\Delta\eta} \bigg/ \frac{1}{N_{\text{pair}}^{\text{mixed}}} \frac{d^2 N_{\text{mixed}}}{d\Delta\phi d\Delta\eta}$$

Pair yields $d^2 N_{\text{pair}}$ corrected for acceptance effects

Mixed sample comprises pairs from different events

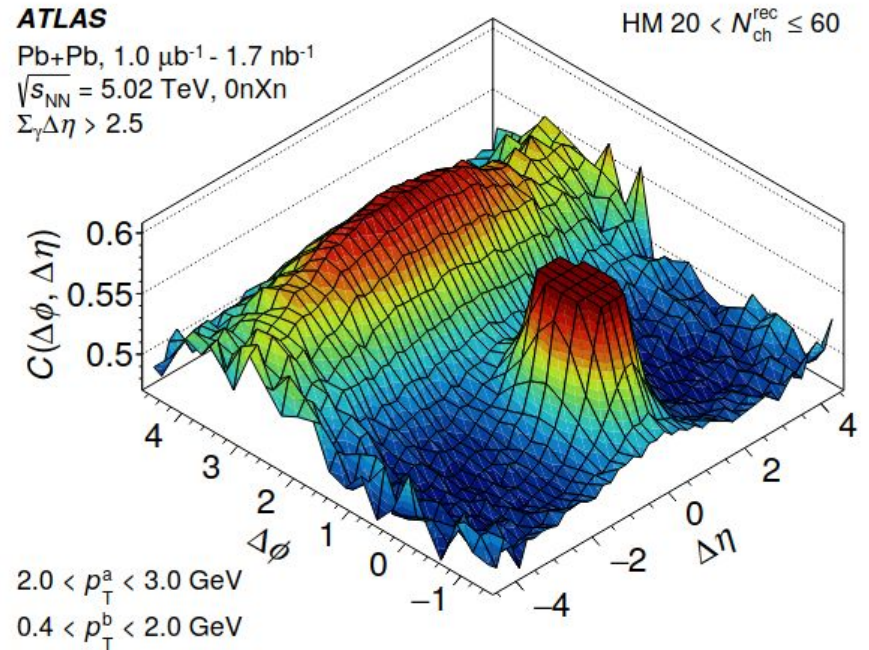
(a) Lower- p_T^a



Away-side ridge $\Delta\phi \approx \pi$

Due to momentum conservation in the transverse plane; a *non-flow* contribution.

(b) Higher- p_T^a



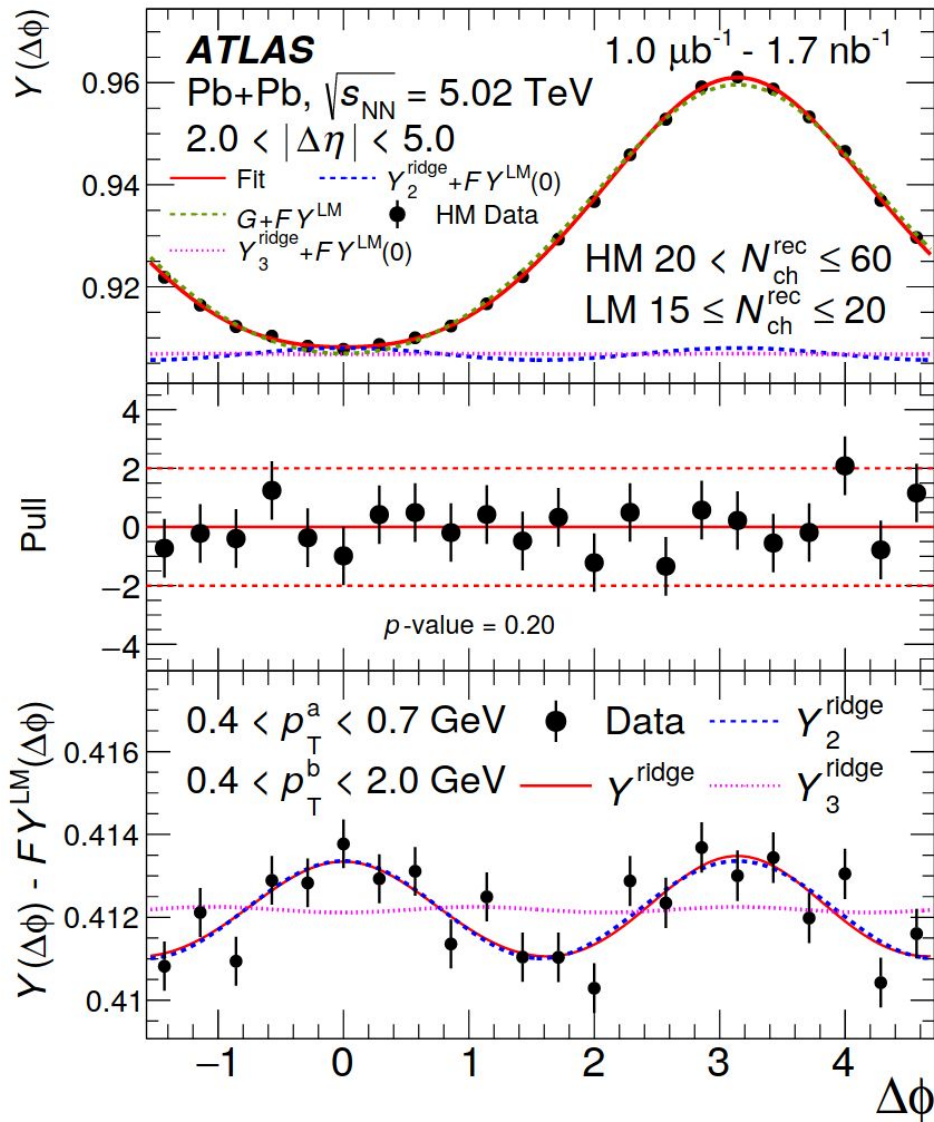
Near-side peak $(\Delta\phi, \Delta\eta) \approx (0, 0)$

From correlations between jet fragments
(Truncated to show other structures)

Non-Flow Subtraction

[2101.10771]

To emphasise the azimuthal modulations due to flow contributions



$$Y^{\text{HM}}(\Delta\phi) = FY^{\text{LM}}(\Delta\phi) + G \left\{ 1 + 2 \sum_{n=2}^4 v_{n,n} \cos(n\Delta\phi) \right\}$$

Size of combinatorial contribution

Azimuthal modulations
 Of the away-side ridge; flow contributions.

Correlation function in Low Multiplicity events

Exhibiting no flow, these events are the template to subtract.
 Free, fourth order Fourier series parameterisation.

To emphasise the azimuthal modulations due to flow contributions

$$Y^{\text{HM}}(\Delta\phi) = FY^{\text{LM}}(\Delta\phi) + G \left\{ 1 + 2 \sum_{n=2}^4 v_{n,n} \cos(n\Delta\phi) \right\}$$

Factorisation assumption

Factor out one of the particles of the two-particle flow coefficient to get *single-particle* flow coefficients.

$$v_n(p_T^a) = v_{n,n}(p_T^a, p_T^b) / v_n(p_T^b) = v_{n,n}(p_T^a, p_T^b) / \sqrt{v_{n,n}(p_T^b, p_T^b)}$$

What about negative v_n ?

Suggests the violation of factorisation and non-flow behaviour

Jet Quenching Analysis

Centrality definition

[2206.01138 (PRL)]

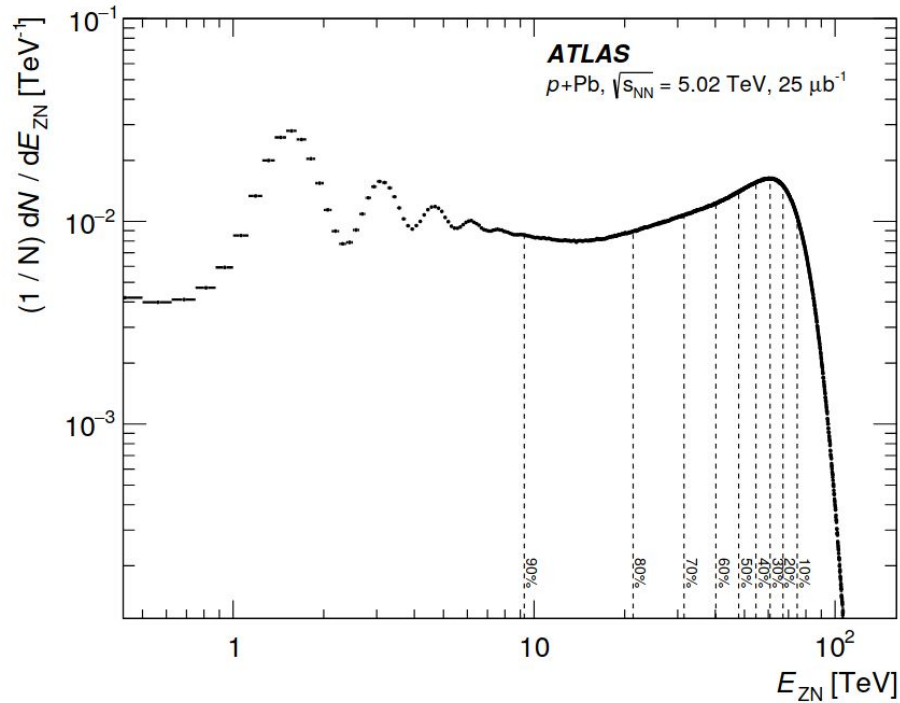
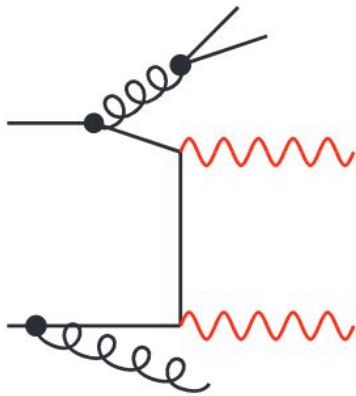


Figure 1: Distribution of energy measured in the Pb-going side of the zero-degree calorimeter (E_{ZN}) in p +Pb collisions at 5.02 TeV selected with a minimum-bias trigger. Dashed vertical lines indicate the percentile boundaries between the 0–10%, 10–20%, etc., centrality intervals.

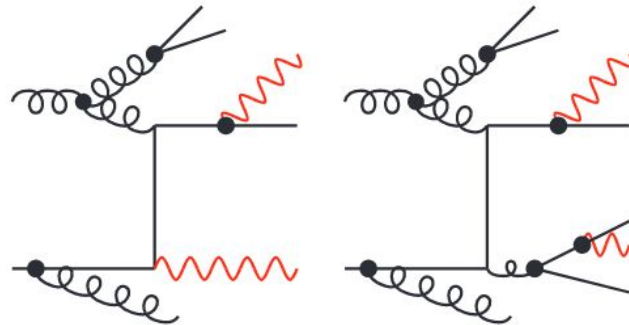
Relevant features of the theory predictions

Table 4: Overview of the theory predictions and their relevant features. The label ‘QCD res.’ (‘NP effects’) stands for QCD resummation (non-perturbative effects).

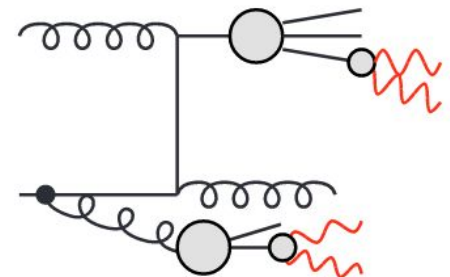
	Fixed-order accuracy					$gg \rightarrow \gamma\gamma$	Fragmentation		QCD res.	NP effects
	$\gamma\gamma$	+1j	+2j	+3j	+ $\geq 4j$		single	double		
DIPHOX	NLO	LO	-	-	-	LO	NLO		-	-
NNLOJET	NNLO	NLO	LO	-	-	LO	-	-	-	-
SHERPA	NLO		LO	PS	LO	ME+PS		PS	✓	



(a) Direct photons



(b) Single- and double-fragmentation photons



(c) Non-prompt photons

Photon selection

Selection	Detector level	Particle level
Photon kinematics	$p_{T,\gamma_{1(2)}} > 40$ (30) GeV, $ \eta_\gamma < 2.37$ excluding $1.37 < \eta_\gamma < 1.52$	
Photon identification	tight	stable, not from hadron decay
Photon isolation	$E_{T,\gamma}^{\text{iso},0.2} < 0.05 \cdot p_{T,\gamma}$	$E_{T,\gamma}^{\text{iso},0.2} < 0.09 \cdot p_{T,\gamma}$
Diphoton topology	$N_\gamma \geq 2$, $\Delta R_{\gamma\gamma} > 0.4$	

★

★ (Photon kinematics)

$p_{T,\gamma}$ cuts 5 GeV above trigger thresholds — in trigger efficiency plateaus

η_γ cuts to operate in region of high EM Calorimeter granularity && exclude barrel–end-cap transition region

Photon Isolation

Cone of $\Delta R = 0.2$ around photon momentum should not have too much transverse momentum in it (Pile-up and Underlying Event contributions corrected for)

Diphoton topology

$\Delta R_{\gamma\gamma}$ cut to prevent overlap between photon isolation cones — reduce correlation between photon isolations)

Photon Pairs analysis

Background estimation

[2107.09330]

For each process $p \in \{\gamma\gamma, \gamma j, j\gamma, jj, ee, \text{pileup}\}$, construct the probability $f_{p,i}$ that an event goes into region i

$$f_{p,i} = f_{p,i}(\varepsilon_{p,1}^{\text{iso}}, \varepsilon_{p,2}^{\text{iso}}, R_p^{\text{iso}}, \varepsilon_{p,1}^{\text{id}}, \varepsilon_{p,2}^{\text{id}}, R_p^{\text{id}}, R_{p,1}^{\text{iso-id}}, R_{p,2}^{\text{iso-id}})$$

		Leading candidate isolation					
		Pass	Fail	Pass	Fail		
Sub-leading candidate identification	Fail	6	8	14	16	Sub-leading candidate isolation	Fail
	Fail	5	7	13	15		Pass
	Pass	2	4	10	12		Fail
	Pass	1	3	9	11		Pass
		Pass	Fail	Leading candidate identification			

$$= \begin{cases} \varepsilon_{p,1}^{\text{iso}} & \varepsilon_{p,2}^{\text{iso}} & \varepsilon_{p,1}^{\text{id}} & \varepsilon_{p,2}^{\text{id}} & \text{for } i = 1 \\ \varepsilon_{p,1}^{\text{iso}} & (1 - \varepsilon_{p,2}^{\text{iso}}) & \varepsilon_{p,1}^{\text{id}} & \varepsilon_{p,2}^{\text{id}} & \text{for } i = 2 \\ (1 - \varepsilon_{p,1}^{\text{iso}}) & \varepsilon_{p,2}^{\text{iso}} R_p^{\text{iso}} & \varepsilon_{p,1}^{\text{id}} & \varepsilon_{p,2}^{\text{id}} & \text{for } i = 3 \\ (1 - \varepsilon_{p,1}^{\text{iso}}) & (1 - \varepsilon_{p,2}^{\text{iso}} R_p^{\text{iso}}) & \varepsilon_{p,1}^{\text{id}} & \varepsilon_{p,2}^{\text{id}} & \text{for } i = 4 \\ \varepsilon_{p,1}^{\text{iso}} & \varepsilon_{p,2}^{\text{iso}} R_{p,2}^{\text{iso-id}} & \varepsilon_{p,1}^{\text{id}} & (1 - \varepsilon_{p,2}^{\text{id}}) & \text{for } i = 5 \\ \varepsilon_{p,1}^{\text{iso}} & (1 - \varepsilon_{p,2}^{\text{iso}} R_{p,2}^{\text{iso-id}}) & \varepsilon_{p,1}^{\text{id}} & (1 - \varepsilon_{p,2}^{\text{id}}) & \text{for } i = 6 \\ (1 - \varepsilon_{p,1}^{\text{iso}}) & \varepsilon_{p,2}^{\text{iso}} R_p^{\text{iso}} R_{p,2}^{\text{iso-id}} & \varepsilon_{p,1}^{\text{id}} & (1 - \varepsilon_{p,2}^{\text{id}}) & \text{for } i = 7 \\ (1 - \varepsilon_{p,1}^{\text{iso}}) & (1 - \varepsilon_{p,2}^{\text{iso}} R_p^{\text{iso}} R_{p,2}^{\text{iso-id}}) & \varepsilon_{p,1}^{\text{id}} & (1 - \varepsilon_{p,2}^{\text{id}}) & \text{for } i = 8 \\ \varepsilon_{p,1}^{\text{iso}} R_{p,1}^{\text{iso-id}} & \varepsilon_{p,2}^{\text{iso}} & (1 - \varepsilon_{p,1}^{\text{id}}) & \varepsilon_{p,2}^{\text{id}} R_p^{\text{id}} & \text{for } i = 9 \\ \varepsilon_{p,1}^{\text{iso}} R_{p,1}^{\text{iso-id}} & (1 - \varepsilon_{p,2}^{\text{iso}}) & (1 - \varepsilon_{p,1}^{\text{id}}) & \varepsilon_{p,2}^{\text{id}} R_p^{\text{id}} & \text{for } i = 10 \\ (1 - \varepsilon_{p,1}^{\text{iso}} R_{p,1}^{\text{iso-id}}) & \varepsilon_{p,2}^{\text{iso}} R_p^{\text{iso}} & (1 - \varepsilon_{p,1}^{\text{id}}) & \varepsilon_{p,2}^{\text{id}} R_p^{\text{id}} & \text{for } i = 11 \\ (1 - \varepsilon_{p,1}^{\text{iso}} R_{p,1}^{\text{iso-id}}) & (1 - \varepsilon_{p,2}^{\text{iso}} R_p^{\text{iso}}) & (1 - \varepsilon_{p,1}^{\text{id}}) & \varepsilon_{p,2}^{\text{id}} R_p^{\text{id}} & \text{for } i = 12 \\ \varepsilon_{p,1}^{\text{iso}} R_{p,1}^{\text{iso-id}} & \varepsilon_{p,2}^{\text{iso}} R_{p,2}^{\text{iso-id}} & (1 - \varepsilon_{p,1}^{\text{id}}) & (1 - \varepsilon_{p,2}^{\text{id}}) R_p^{\text{id}} & \text{for } i = 13 \\ \varepsilon_{p,1}^{\text{iso}} R_{p,1}^{\text{iso-id}} & (1 - \varepsilon_{p,2}^{\text{iso}} R_{p,2}^{\text{iso-id}}) & (1 - \varepsilon_{p,1}^{\text{id}}) & (1 - \varepsilon_{p,2}^{\text{id}}) R_p^{\text{id}} & \text{for } i = 14 \\ (1 - \varepsilon_{p,1}^{\text{iso}} R_{p,1}^{\text{iso-id}}) & \varepsilon_{p,2}^{\text{iso}} R_p^{\text{iso}} R_{p,2}^{\text{iso-id}} & (1 - \varepsilon_{p,1}^{\text{id}}) & (1 - \varepsilon_{p,2}^{\text{id}}) R_p^{\text{id}} & \text{for } i = 15 \\ (1 - \varepsilon_{p,1}^{\text{iso}} R_{p,1}^{\text{iso-id}}) & (1 - \varepsilon_{p,2}^{\text{iso}} R_p^{\text{iso}} R_{p,2}^{\text{iso-id}}) & (1 - \varepsilon_{p,1}^{\text{id}}) & (1 - \varepsilon_{p,2}^{\text{id}}) R_p^{\text{id}} & \text{for } i = 16. \end{cases}$$

$$n_i^{\text{exp}} = \frac{n_{\gamma\gamma}}{\varepsilon_{\gamma\gamma,1}^{\text{id}} \varepsilon_{\gamma\gamma,1}^{\text{iso}} \varepsilon_{\gamma\gamma,2}^{\text{id}} \varepsilon_{\gamma\gamma,2}^{\text{iso}}} f_{\gamma\gamma,i} + N_{\gamma j} f_{\gamma j,i} + N_{j\gamma} f_{j\gamma,i} + N_{jj} f_{jj,i} + N_{ee} f_{ee,i} + N_{\text{PU}} f_{\text{PU},i}$$